



## OPEN The variation rule of TBM tunneling parameters in deep composite strata and the recognition method of boreability grade

Haibin Wang<sup>1</sup>, Guogang Cui<sup>1</sup>, Zhen Shi<sup>1</sup>, Ling Zhang<sup>1</sup>, Chengdeng Gao<sup>2</sup>✉ & Ziwei Ding<sup>2</sup>

To evaluate the energy efficiency of tunneling with an open full-section road header constructed in deep coal composite strata, this study relies on the development project of the 1# backdraft tunnel in the western area of a mine located in Binchang, Shaanxi Province. The analysis is based on machine-rock data collected by the Tunnel Boring Machine (TBM) while excavating through various composite strata, including muddy sandstone layers, muddy sandstone and coal composite strata, coal strata, medium-coarse sandstone layers, medium-coarse sandstone, and fine sandstone composite stratum, fine sandstone stratum. Descriptive statistics, correlation analysis, regression analysis, and other Mathematical and statistical methods are used to analyze the change rule of TBM tunneling parameters in different formations, and the optimized regulation range of tunneling parameters is proposed. At the same time, the propulsion factor, tunneling speed, and tunneling specific energy are introduced as the boreability evaluation indexes, and a quantitative identification method of formation boreability level is established to reasonably classify the difficulty level of tunneling in different formations. The results show that: (1) the change characteristics of five main tunneling parameters in different formations are obtained through data preprocessing, and the change trends of tunneling speed and penetration in different formations are consistent, while the change trends of cutter speed, thrust, and torque are opposite to that of penetration. (2) The main tunneling parameters in different formations are analyzed by numerical statistics, and it is found that all of them are normally distributed, and the 25% and 75% position of data distribution is taken to the values of 25% and 75% of the data distribution are given, and the reasonable regulation range of each parameter is given. (3) The two characteristic parameters of thrust factor and tunneling specific energy are introduced to analyze the tunneling energy efficiency of TBM tunneling in different strata, and the variation of the characteristic parameters in a single stratum is small, and the oscillatory nature of them in composite strata is significantly higher than that of a single stratum by a factor ranging from 1.29 to 3.64. (4) The identifying method of the tunneling grade of a strata has been established based on the indicators of the tunneling speed and the energy consumption of tunneling, and a characteristic parameter is proposed to identify the level of the tunneling performance. The identification method of grade is established based on the index of tunneling speed and energy consumption, and the fluctuation correction factor of characteristic parameter is proposed to quantitatively evaluate the degree of difficulty of tunneling in six kinds of strata. The stratum boreability grade identification method proposed in this paper can effectively classify the composite strata under deep and complex geological conditions, and provide important reference and guidance for the assessment and prediction of stratum boreability and optimization of tunneling parameter control in the smooth running section of TBM.

**Keywords** Tunneling parameters, Thrust factor, Special energy, Boreability analysis

The tunneling parameters serve as the state response of a Tunnel Boring Machine (TBM) when tunneling into the formation, and again the performance of TBM in the formation. Therefore, the tunneling parameters of the TBM across different strata are collected through sensor monitoring, to map out the current state of

<sup>1</sup>Shandong Energy Group Northwest Mining Co., Ltd., Xi'an 710021, Shaanxi, China. <sup>2</sup>College of Energy and Mining Engineering, Xi'an University of Science and Technology, Xi'an 710054, Shaanxi, China. ✉email: xustgcd@163.com

excavation in the strata and optimize the parameters, to improve the construction efficiency and safety<sup>1,2</sup>. Deep coal strata present complex and variable geological conditions. Although the coal beds are primarily composed of sedimentary rocks, the undulation of these beds leads to the coal beds, different strata, and various types of composite strata during underground roadway excavation<sup>3–5</sup>. The drilling performance of a TBM is influenced by a range of geological conditions; therefore, accurately assessing the boreability of the rock and optimizing the drilling parameters is a critical issue in TBM construction<sup>6</sup>.

In the process of TBM tunneling, the excitability grade of the tunnel surrounding the rock is affected by many factors, among which the most important parameter is the real-time perception parameter of the rock body. There are two main ways to obtain rock parameters: laboratory mechanical experiments and data export from the onboard system. In terms of laboratory mechanical experiments, the mechanical parameters of the rock body are obtained by drilling standard specimens of different lithologies on-site and conducting mechanical experiments on intact specimens or specimens containing fissure holes<sup>7–10</sup>. Numerical models are established for mechanical property inversion based on the existing mechanical parameters, and machine learning algorithms carry out mechanical parameter prediction to realize the perceptual recognition of the rock body state<sup>11–13</sup>. Although indoor mechanical experiments have achieved good results in the acquisition of rock body parameters, due to the complexity and variability of the rock layers in coal mine TBM excavation, it is not possible to collect rock samples in front of TBM excavation in real time for mechanical experiments, and there is an obvious lag. Compared with indoor mechanical experiments, the tunneling parameter identification method has higher practicality and accuracy and can provide timely feedback for each kind of lithology change.

In recent years, domestic and foreign scholars have conducted studies on TBM tunneling parameter optimization and rock mass drivability evaluation. Based on the analysis of the evolution law of tunneling parameters in the whole section of gravel sand, weathered shaly siltstone, and sand-rock composite strata in the whole section of shield excavation, Wang et al.<sup>14</sup> carried out the correlation analysis of the main tunneling parameters, to qualitatively evaluate the drivability of the strata. Yang et al.<sup>15</sup> focused on the adaptability of EPB/TBM dual-mode shield tunneling in composite strata, discussed the variation law and correlation of tunneling parameters under different tunneling modes and optimized the control range of tunneling parameters. He et al.<sup>16,17</sup> compared the adaptability of EPB/TBM dual-mode shield tunneling in different strata, analyzed the tunneling parameters and energy consumption under different tunneling modes and provided a theoretical basis for the prediction and decision optimization of tunneling parameters. Xia et al.<sup>18</sup> analyzed the correlation between cutter head speed, total thrust, and tunneling speed in six kinds of lithologic strata, and gave the reasonable control interval of three parameters by mathematical statistics. Based on the analysis of shield tunneling parameters in composite strata, Zhao et al.<sup>19</sup> found that the total thrust had the largest fluctuation in hard rock strata, while the average advance speed was the lowest in granite differential weathering and hard rock strata. Huang et al.<sup>20</sup> proposed the effective specific thrust index EFPI considering the influence of soil chamber pressure, which was used to characterize the change of formation conditions and analyze the evolution law of shield tunneling parameters. The results show that EFPI is superior to the traditional FPI index in evaluating the difficulty of shield cutting surrounding rock, and has a linear positive correlation with the number of standard penetration shots. Duan et al.<sup>21</sup> studied the relationship between tunneling parameters of single shield TBM in sandstone and sandy mudstone strata. Through statistical analysis, the recommended values of tunneling parameters under normal tunneling conditions were obtained, and the relationship between tunneling speed and tunneling parameters was fitted. Based on the TBM tunneling performance, Wu et al.<sup>22</sup> established the rock mass drivability classification and the drivability grade perception recognition method. The TOPSIS multi-objective decision-making method is used to realize the classification of rock mass drivability, and the accurate perception and recognition of rock mass drivability grade is realized by using the machine learning classification model of Bayesian optimization and TBM tunneling parameters. Wu et al.<sup>23</sup> divided the rock mass drivability into six categories by K-center cluster analysis method and discussed the distribution law of TBM average single cutter thrust and cutter head speed under different rock mass drivability conditions, which guided the evaluation of rock mass drivability and the selection of tunneling parameters in TBM construction tunnel. Zhang et al.<sup>24</sup> proposed a rock mass state perception method based on TBM tunneling process monitoring to solve the problem that the rock mass state parameters of the TBM tunnel face are difficult to obtain in real-time. The database of TBM tunneling parameters and rock mass parameters is established, and the model of the rock mechanism system is established by step-by-step regression and cluster analysis, which realizes the real-time perception of rock strength, volume joint number, and surrounding rock grade. Aiming at the problem of real-time identification of stratum characteristics in shield tunneling, Qiao<sup>25</sup> proposed a stratum category prediction model based on a machine learning algorithm. The model uses the correlation between shield construction parameters and geological characteristics and establishes the relationship between shield construction parameters and stratum categories through the CART decision tree and random forest algorithm, which provides a new method for the classification and prediction of stratum categories during shield tunneling. Zhang et al.<sup>26</sup> focused on the timely identification of the state of broken surrounding rock in TBM tunneling of coal mine roadway and proposed a method for identifying the characteristics of surrounding rock based on tunneling parameters. By analyzing the correlation and recognition ability of tunneling parameters, this method uses the LSTM model to predict and effectively identify the broken state of surrounding rock, which is of great significance to construction safety. Xie et al.<sup>27</sup> proposed a comprehensive classification method of surrounding rock based on tunneling performance in TBM construction. This method comprehensively considers the excavation ability of surrounding rock and the adaptability of TBM. Taking the construction speed as the index, a new method of surrounding rock classification for TBM tunnel engineering is established, which provides a new perspective for the classification of surrounding rock in TBM construction. In summary, the correlation analysis between TBM tunneling parameters and lithological strata is very important for construction efficiency and safety. The existing research mostly focuses on the parameter optimization of single stratum or composite stratum under specific engineering

conditions in shallow stratum tunnel engineering. However, the optimization of tunneling parameters and the evaluation of rock drivability under the condition of a composite stratum of coal measures in a kilometer-deep well still need further research.

Based on the 1# return air development roadway project in the west area of a mine in Binchang, Shaanxi Province, this paper makes a statistical analysis of the main tunneling parameters of the open full-face TBM in shaly sandstone layer, shaly sandstone, and coal seam composite stratum, coal seam, medium coarse sandstone layer, medium coarse sandstone and fine sandstone composite stratum, and fine sandstone stratum. Taking thrust factor, tunneling speed, and tunneling specific energy as the indexes of stratum drivability, the tunneling energy efficiency performance of TBM in six different strata is carried out, to provide parameter control guidance for TBM construction in composite strata under deep complex geological conditions.

Engineering situations  
Engineering background

The 1# return air development roadway in the western area of a mine in Binchang, Shaanxi is located in the south of Qimagou Village and Jinghe River, just above Sijiahe Village. The ground elevation is + 929.80 ~ + 1040.30 m, the design length is 5204 m, 132 m from the 1205 contact roadway, the azimuth angle is 305°, the slope is 5‰, the tunneling is 513 m, the direction is adjusted to the azimuth angle of 299°, the construction is 791 m according to 5‰, then the construction is 388 m according to 6‰, and the construction is 3512 m according to 5‰ to the design boundary. EQC6330 open-type full-face TBM is used for TBM tunneling, and the design section diameter is 6.33 m. Due to the need to cross hard rock strata such as fine sandstone and medium-coarse sandstone, the cutter head steel structure is made of Q345D material. The cutter head panel is welded with SA1750CR wear-resistant composite steel plate, and the outer ring is welded with an inlaid alloy wear-resistant plate. There are 38 high-quality tool steel hobs installed, which can withstand a maximum load of 250kN and a maximum rock-breaking capacity of 200 MPa. In the process of TBM tunneling, the information parameters of the on-site roadway tunneling state can be obtained in real-time and selectively. The cutter head structure type and the main technical parameters of the equipment are shown in Table 1.

Engineering geological and stratigraphic characteristics

The geological conditions of the 1# backwind open-up alley in the west area are shown in Fig. 1. According to the engineering design, the tunnel is expected to expose the strata mainly as sandy mudstone and fine-medium sandstone composite strata, sandy mudstone and fine sandstone composite strata, muddy fine sandstone and 4# coal composite strata, sandy mudstone and fine sandstone composite strata, alumina mudstone, medium-coarse sandstone, and fine sandstone composite strata, and mudstone. To study the variation law of TBM tunneling parameters in different hardness lithology, hard rock, hard rock interbedded, hard rock and soft rock interbedded, soft rock is medium coarse sandstone, fine sandstone, medium coarse sandstone and fine sandstone interbedded, shaly fine sandstone, shaly fine sandstone and coal interbedded, 4# coal seam 6 kinds of strata tunneling parameters were studied and analyzed. The selected soft and hard interbedded research area first passes through the whole section of shaly fine sand stratum (about 127 m); TBM began to excavate shaly fine sandstone and 4# coal composite strata (about 66 m) when TBM tunneling to 665.55 m. With TBM tunneling, the proportion of soft rock coal seam in the upper part of the excavation section increased continuously until 731.55 m TBM began to tunnel in the whole section of the coal seam. The hard rock interbedded area is selected to pass through the medium-coarse sandstone layer (about 60 m) in the whole section, and then enter the

Cutterhead structure type	Parameters	Values
	TBM type	open-type
	Cutterhead diameter <i>D</i> (mm)	6330
	Cutterhead speed (r·min <sup>-1</sup> )	0 ~ 7.1
	Cutterhead torque <sub>max</sub> (kN·m)	2830
	Extricating torque (kN·m)	4250
	Disc cutter number	38
	Propulsion cylinder stroke (mm)	1829
	Slag discharge capacity (t·h <sup>-1</sup> )	600
	Maximum ground specific pressure (MPa)	< 3
	Effective support force of boots (kN)	38,150
	Advance displacement (mm)	> 1200
	Adapt to maximum slope (°)	± 6
	Minimum horizontal turning radius (m)	500
	Maximum particle size allowed to be conveyed (mm)	200
	Cutterhead thrust <sub>max</sub> (kN)	19,782

Table 1. The main technical parameters of TBM.

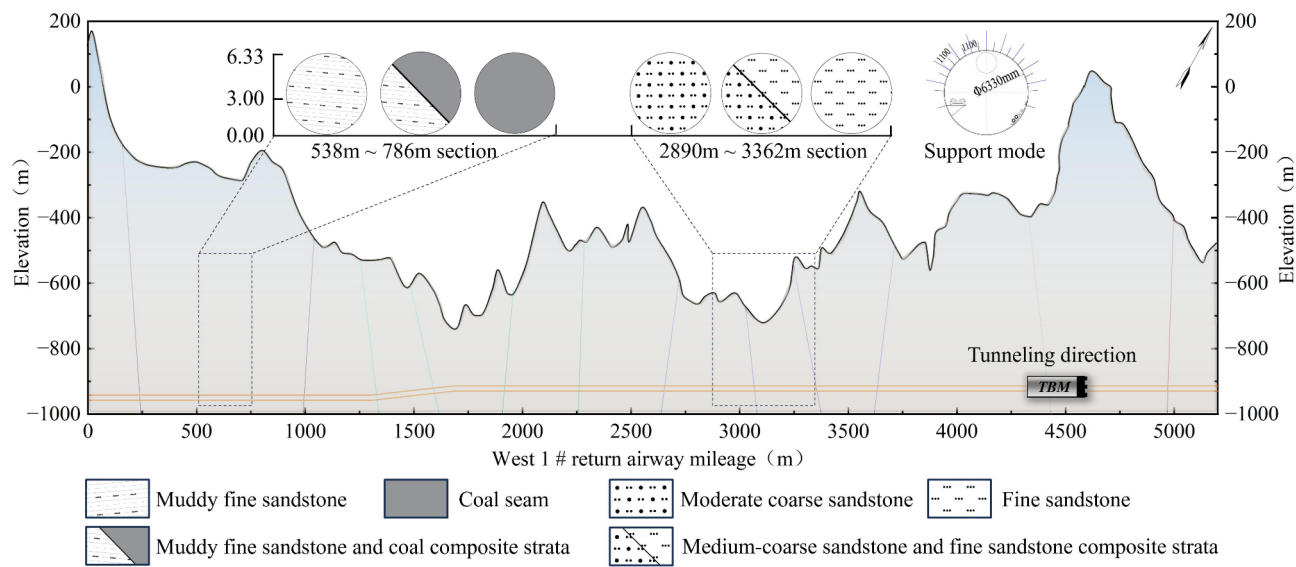


Fig. 1. Geological profile of 1# return airway in the western district.

Rock type	Natural unit weight (g·cm <sup>-3</sup> )	Porosity	Moisture content (%)	Dry compressive strength (MPa)	Saturated compressive strength (MPa)	Elastic modulus (×10 <sup>4</sup> MPa)	Poisson's ratio	Cohesion (MPa)	Tensile strength (MPa)
Shaly sandstone	2.56	6.21	1.53	30.14	19.82	1.417	0.23	3.38	1.50
4# coal seam	1.52	7.27	4.47	15.26	9.60	0.537	0.25	1.67	0.47
Medium-coarse sandstone	2.52	7.96	0.97	43.23	28.72	1.488	0.23	3.25	1.65
Fine sandstone	2.50	8.92	1.06	32.71	22.72	1.659	0.23	3.43	1.51

Table 2. The main physical and mechanical parameters of rock strata in the selected area.

composite stratum of medium-coarse sandstone and fine sandstone. With the advancement of TBM, the proportion of medium-coarse sandstone at the bottom of the excavation section decreases continuously, and the total length of the composite stratum of medium-coarse sandstone and fine sandstone is about 112 m.

According to the occurrence characteristics and formation conditions of the mined aquifer, the roadway excavation is mainly affected by the Jurassic Yan'an Formation-coarse grained sandstone and the Triassic Hujiacun Formation sandy mudstone fissure aquifer. The water-filling method is roadway seepage and roof watering, which belongs to the weak water-rich aquifer and can be gradually drained with head-on excavation. The normal water inflow is expected to be 27.5 m<sup>3</sup>·h<sup>-1</sup>, and the maximum water inflow is 41.3 m<sup>3</sup>·h<sup>-1</sup>.

According to the geological prospecting report, the coal uncovering section in the selected research area is the 4# coal seam of Yan'an Formation, which is a single thick coal seam with a thickness of 8.60~15.80 m, an average of 12.93 m, and a coal seam dip angle of 0°~14°, with an average dip angle of 7°. The medium-coarse sandstone and fine sandstone are light gray-white, mainly quartz, and feldspar, with thin mudstone layers in some areas. The shaly fine sandstone is light gray, with flat sections and horizontal bedding. The physical and mechanical parameters of different strata in the selected area are shown in Table 2.

TBM tunneling data characteristics and preprocessing  
Selection of TBM tunneling parameters

In the process of TBM tunneling, real-time data acquisition is carried out by speed sensor, oil pressure sensor, and stroke sensor, including propulsion system parameters, hydraulic fluid system parameters, cutter head motor parameters, guidance system parameters, and auxiliary system parameters. It mainly includes tunneling speed, penetration, total propulsion, cutter head speed, cutter head torque, left and right support boots tightening pressure, left and right support boots displacement, host belt drive pressure, left and right shield displacement, etc., a total of 57 data acquisition. Most of the parameters are set values, and only a small part of the rock breaking is related to the change of the excavation strata. It can be divided into active control parameters (Cutterhead speed *n* and Tunneling speed *v*), passive performance parameters (Total thrust *F* and Cutterhead torque *T*), and target parameters (Penetration *P*).

According to the range of crossing strata, the tunnel mileage of 538–665 m is taken as the tunneling data when TBM passes through the whole section of shaly fine sandstone, the tunnel mileage of 666–731 m is taken as the tunneling data when TBM passes through the coal-rock composite stratum, the tunnel mileage of 732–786 m is taken as the tunneling data when TBM passes through the whole section of coal seam, the tunnel mileage of



2890–2950 m is taken as the tunneling data when TBM passes through the whole section of medium-coarse sandstone, and the tunnel mileage of 2951–3062 m is taken as the tunneling data when TBM passes through the medium-coarse-fine sandstone composite stratum. The tunnel mileage of 3063–3362 m is the tunneling data when TBM passes through the whole section of fine sandstone. According to the change of strata, the parameters corresponding to lithology in 6 cases were selected for statistical analysis, and a total of 99,012 groups of field excavation data were collected.

### Tunneling parameter pretreatment

The sampling time interval of the time domain signal in the roadway excavation process is 1 min, and there are a large number of non-stable phase data such as shutdown data, start-stop phase data, and transmission anomaly data in the real-time collected TBM excavation data, and the different data corresponding to the different phases of the cycle of excavation in different stages of the excavation state, which mainly includes the empty push phase, the ascending phase, the stable excavation phase, the descending phase, and the shutdown phase, as shown in Fig. 2. The raw data in the non-stabilized tunneling stage has a huge amount of data, and the fluctuation of the value change is large on the overall data change law also produces greater interference. Before researching the change rule of TBM tunneling parameters in different strata, it is necessary to eliminate the invalid data collected continuously from the original data and splice the stable stage data to get the stable stage data.

In order to exclude the data in the stopping section and the empty pushing section, a binary discriminant function is used to discriminate, and in the same set of data collected at a certain sampling point, if one of the four parameters of cutter thrust, tunneling speed, cutter torque, and cutter rotational speed is zero, the data in the set will be excluded<sup>28</sup>.

$$f(x) = f(F) \cdot f(v) \cdot f(T) \cdot f(n) \quad (1)$$

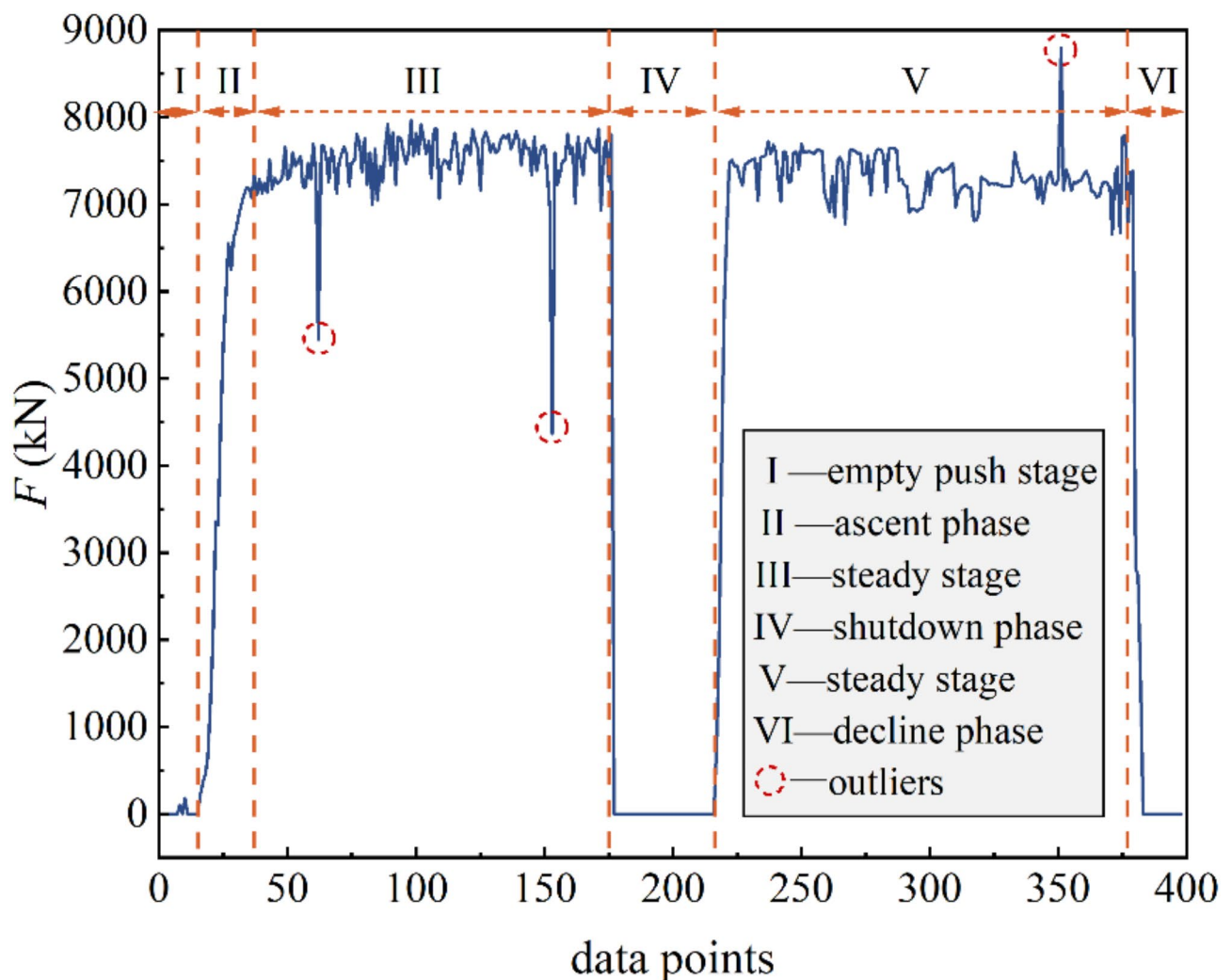


Fig. 2. Time history curve of local cyclic tunneling parameters.

$$f(x) = \begin{cases} 1 & (x \neq 0) \\ 0 & (x = 0) \end{cases} \quad (2)$$

where  $F$  is the TBM cutter thrust, kN;  $v$  is the propulsion speed,  $\text{mm} \cdot \text{min}^{-1}$ ;  $T$  is the cutter torque, kN m;  $n$  is the cutter rotational speed,  $\text{r} \cdot \text{min}^{-1}$ ; and  $f(x)$  is the discriminant function.

For the outliers in the raw data, the box-and-line plot quartile method was used for the identification of abnormal data, using the quartile distance as the basis for the judgment of the outliers, and the box-and-line plot consists of three main parts: box, box whiskers, and outliers, as shown in Fig. 3. After eliminating the outliers in the original number using the box-and-line diagram, smoothing was applied to the missing values, i.e., replacing these outliers with the average of the surrounding five neighboring data<sup>29</sup>.

$$IQR = \frac{Q_3 - Q_1}{2} \quad (3)$$

$$UEV = Q_3 + 1.5 \cdot IQR \quad (4)$$

$$LEV = Q_1 - 1.5 \cdot IQR \quad (5)$$

where  $Q_3$  is the upper quartile,  $Q_1$  is the lower quartile,  $IQR$  is the lower quartile difference,  $UEV$  is the upper boxwhisker, and  $LEV$  is the lower boxwhisker.

The period from contacting the cutting face to stabilizing the cutting parameters of the TBM cutter is the rising stage, the period when the cutting parameters remain stable and slightly fluctuate is the stabilizing stage, and the period from stabilizing the cutting state to the stopping state is the declining stage. The performance of the stabilized section is a key factor in measuring the efficiency and safety of TBM, so this paper selects the stabilized section of the tunneling parameters in the tunneling cycle stage for research. Based on the standard deviation of the oscillation amplitude between the set value of propulsion speed  $v_{\text{set}}$  and the actual speed  $v$  as a criterion whether to enter the stabilization stage, i.e., to meet the real-time data division criterion  $\sigma_s$  is greater than or equal to the standard deviation of the data  $\sigma$  of the set value of  $v_{\text{set}}$  and set the starting  $v_{\text{set}} = 10\%$ , the

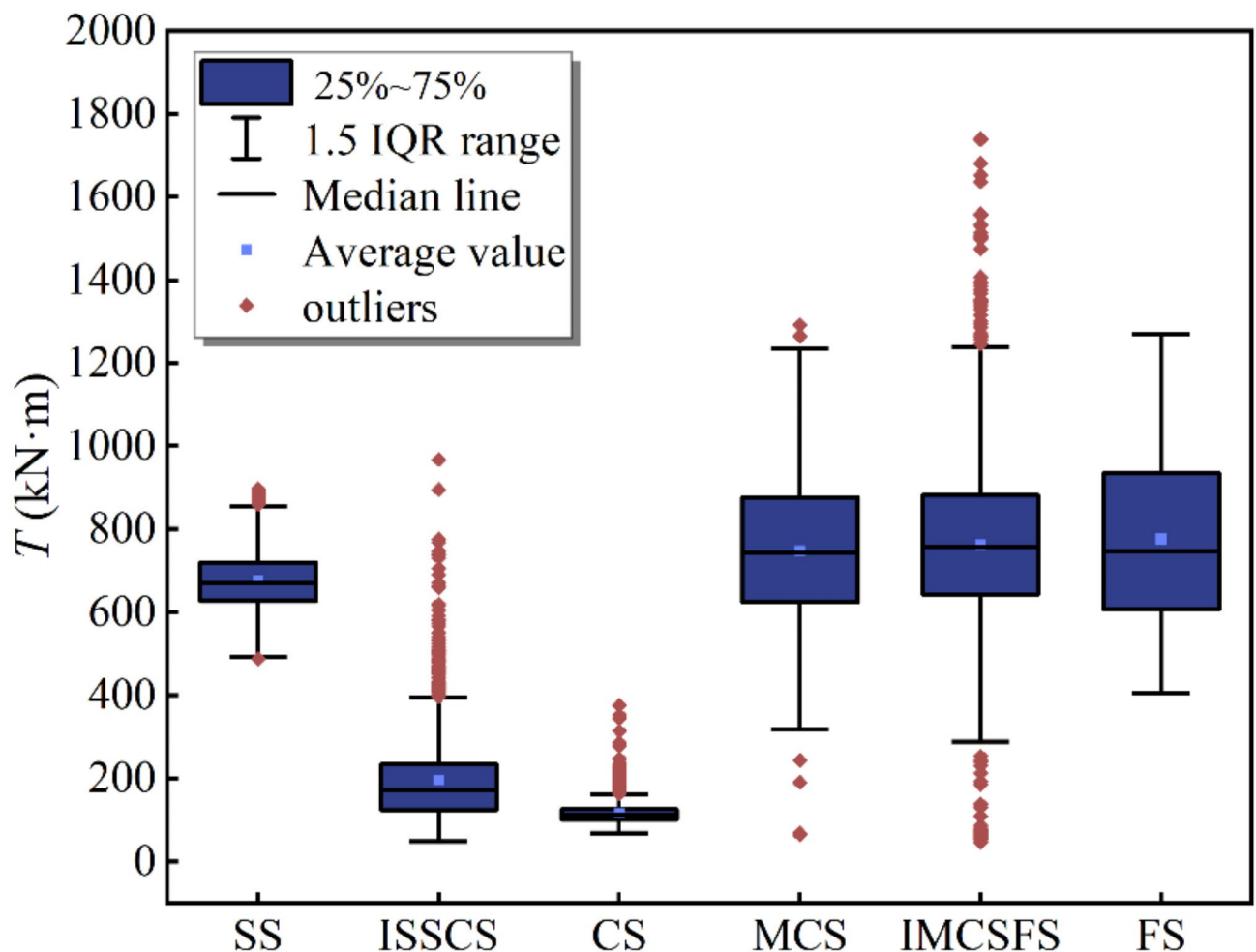


Fig. 3. Box plots of TBM cutter head torque parameters for different formations.

standard deviation of  $\sigma_s$  is regarded as a valid step when it is longer than 60s, it is judged that the TBM enters the stabilization stage of the tunneling<sup>30</sup>.

$$\sigma \leq \sigma_s \quad (6)$$

$$\sigma_s = \sqrt{\frac{\sum_{i=1}^N (x_i - \bar{x})^2}{N}} \quad (7)$$

where  $x$  is the set speed value;  $\bar{x}$  is the mean value;  $N$  is the number of samples.

The original tunneling parameters are shown in Fig. 4a, and the tunneling parameters under steady state are obtained by the above preprocessing method, as shown in Fig. 4b. In the field tunneling data acquisition process, due to the complex tunneling environment, the signal jitter is serious and there is a lot of noise in the data. Therefore, smoothing is utilized to process the outlier and noisy data to obtain the trend of the tunneling parameters over time<sup>31</sup>, as shown in Fig. 4c. From the results before and after the cutter thrust data processing, it is more continuous and intuitive to reflect the change rule of tunneling parameters with geology in the process of tunneling to provide a data basis for the correlation analysis between tunneling parameters and strata.

### Correlation analysis of tunneling parameters

The Pearson correlation coefficient is used to analyze the correlation between the two parameters. The calculation formula is as shown in Eq. (8). The Pearson correlation coefficient is a measure of the linear relationship between the two parameters. If the value is regular, it indicates a positive correlation. Conversely, if the value is negative, it indicates a negative correlation. The closer the absolute value is to one, the stronger the correlation is. The calculation results of the *Pearson* correlation coefficient between the two parameters of TBM are shown in Fig. 5.

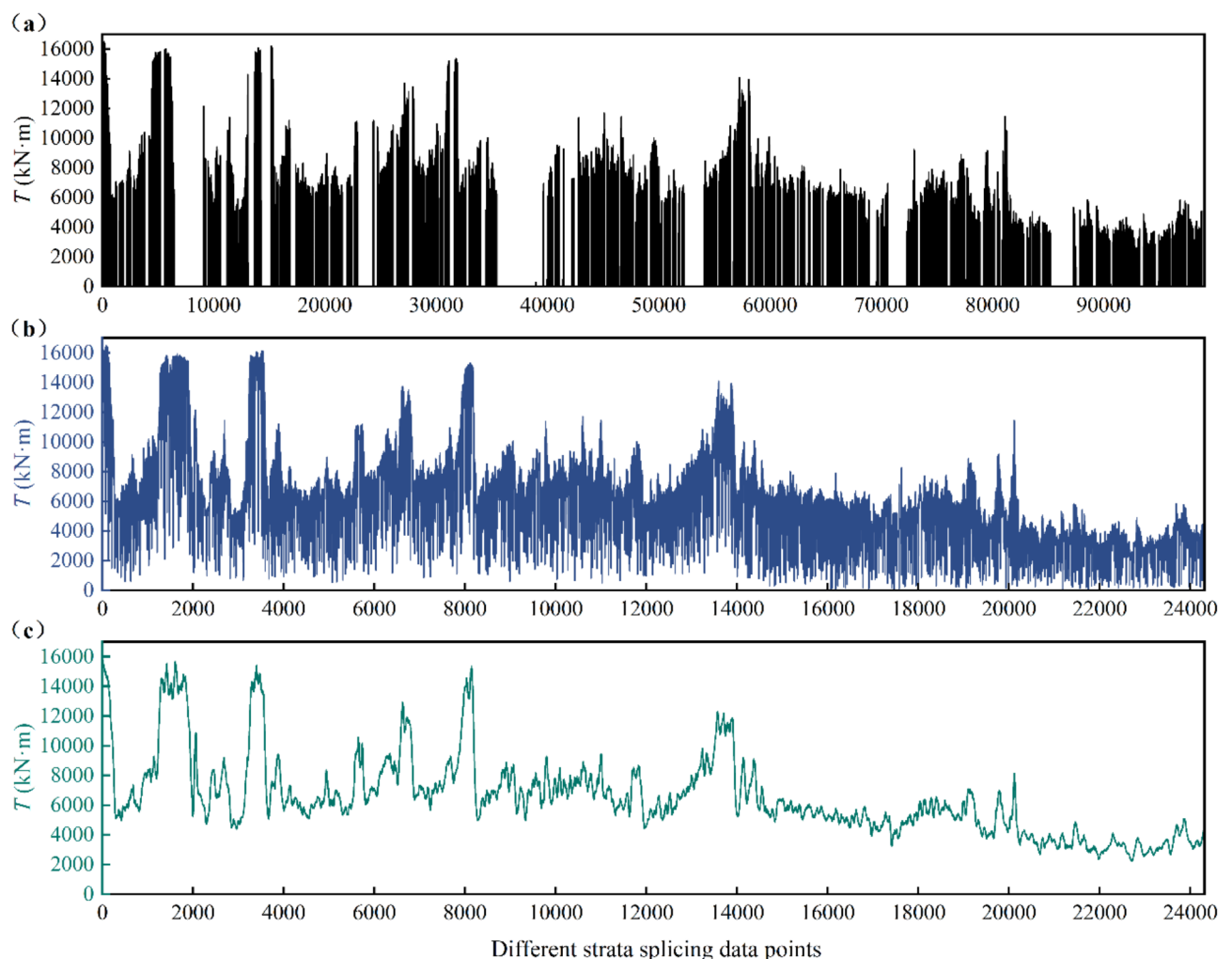


**Fig. 4.** Comparison of the total thrust before and after data processing. (a) Initial total thrust; (b) Total thrust after data preprocessing; (c) Total thrust after smoothing

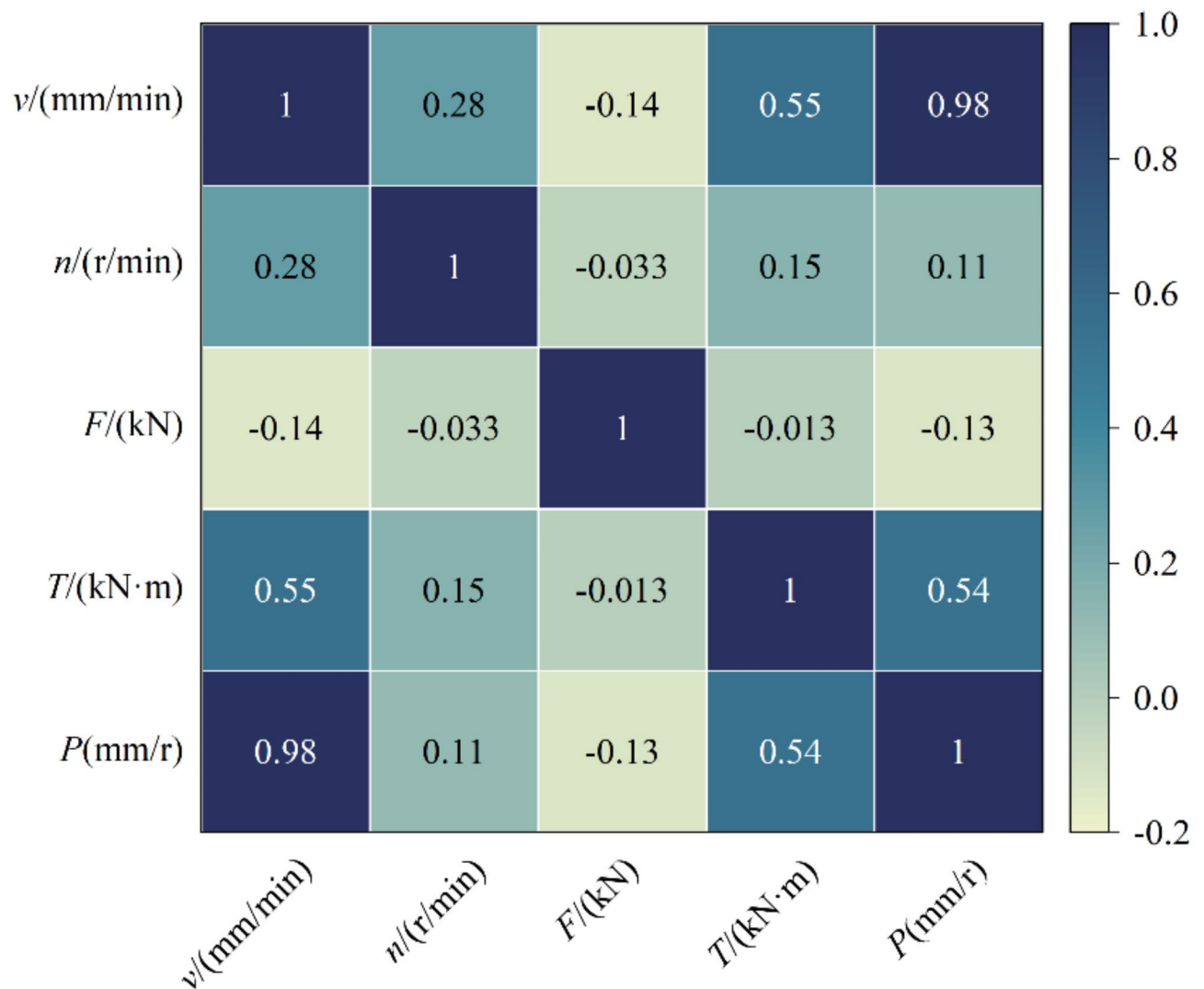


**Fig. 5.** Correlation matrix of TBM tunneling data.

$$r = \frac{N \sum x_i y_i - \sum x_i \sum y_i}{\sqrt{N \sum x_i^2 - (\sum x_i)^2} \sqrt{N \sum y_i^2 - (\sum y_i)^2}} \quad (8)$$

In the formula:  $x$ , and  $y$  are the values of the two variables of the  $i$  the sample;  $N$  is the number of samples.

Through the correlation matrix of Fig. 5, the relationship between different parameters of TBM tunneling can be well analyzed. In addition to the negative correlation with the total thrust, the penetration of the target parameter is positively correlated with other parameters. The correlation between tunneling speed ( $v$ ) and penetration ( $P$ ) is the strongest, and the correlation coefficient reaches 0.98. There is also a strong correlation between cutter head torque and tunneling speed and penetration, and the correlation coefficient is more than 0.5. There is a certain degree of correlation between tunneling speed and cutter head speed, cutter head speed and cutter head torque, penetration, and other parameters, and the correlation coefficient exceeds 0.1. In general, there is a complex coupling relationship between the parameters. Each parameter has important practical significance and theoretical basis for a specific engineering background because each parameter contains only information from this engineering background. Therefore, it is necessary to analyze the variation law of the parameters in TBM tunneling more comprehensively for further analysis.

### The variation law of tunneling parameters in different lithology strata

#### The variation law of TBM active control parameters

##### Tunneling speed

Tunneling speed is the distance the TBM digs forward in a unit of time, usually measured in millimeters per minute ( $mm \cdot min^{-1}$ ). Tunneling speed can be measured by the stroke sensor of the propulsion cylinder. The sensor detects the expansion and contraction stroke of the propulsion cylinder and calculates the tunneling



speed in combination with the time. The variation rule of the tunneling speed parameter in different lithologies and their composite strata is shown in Fig. 6. The Coefficient of Variation (CV) is used to describe the degree of dispersion of the tunneling parameters, and the smaller the value of the coefficient of variation, the more stable the data. As shown in Fig. 6a, there are significant differences in the tunneling speed of different types of rock strata in the tunneling process. The difference in rock strength in a single rock formation is relatively small, its amplitude is small, the coefficient of variation is 0.07~0.14, and the data are relatively stable; in composite formation, due to the change in the strength of soft and hard rock layers in the boring section, the amplitude of the oscillation of the boring speed parameter is increased, and the coefficient of variation is 0.22~0.23, and the data have a large degree of dispersion.

As shown in Fig. 6b, c, the tunneling speed in different strata is normally distributed. Except that there are multiple concentrated distributions in the interbedded of shaly sandstone and coal seam, the other strata belong to a single distribution, and the quartile ranges are 30.15~33.46, 23.20~31.83, 23.12~28.07, 17.66~21.58, 20.11~27.06 mm·min<sup>-1</sup> and 24.83~29.36 mm·min<sup>-1</sup>, respectively. It can be seen from the median of the tunneling speed parameters: shaly sandstone formation>shaly sandstone and coal seam interbedded>fine sandstone formation>coal seam>fine sandstone and medium coarse sandstone interbedded>medium coarse sandstone formation. On the whole, the weak coal seam and hard medium-coarse sandstone have the slowest driving speed, and good driving speed is achieved in shaly sandstone and fine sandstone. The highest average speed is 31.7 mm·min<sup>-1</sup>, and the driving in the interbedded strata is between the two lithologies. It can be seen that the rock strength is the main factor affecting the tunneling speed, and the most suitable rock strength is about 30 MPa. The tunneling speed varies greatly in different strata, so the recommended tunneling speed control ranges in the six strata are: 30~33 mm·min<sup>-1</sup>, 23~31 mm·min<sup>-1</sup>, 25~29 mm·min<sup>-1</sup>, 18~28 mm·min<sup>-1</sup>, 20~27 mm·min<sup>-1</sup> and 18~22 mm·min<sup>-1</sup>.

#### Cutterhead speed

Cutter speed is the number of revolutions per minute that a cutter rotates, usually measured in revolutions per minute (r·min<sup>-1</sup>). The rotational speed of the cutterhead can be measured by a rotational speed sensor mounted on the drive shaft of the cutterhead. The sensor detects the rotational speed of the cutterhead and converts it into a specific RPM value. The changing law of the cutter rotational speed parameter in different lithologies and their composite formations is shown in Fig. 7. As shown in Fig. 7a, the amplitude of the change of the cutter rotational speed in different types of rock strata in the process of tunneling is not large, its amplitude is small, and the coefficients of variation are less than 0.10, so the data are relatively stable.

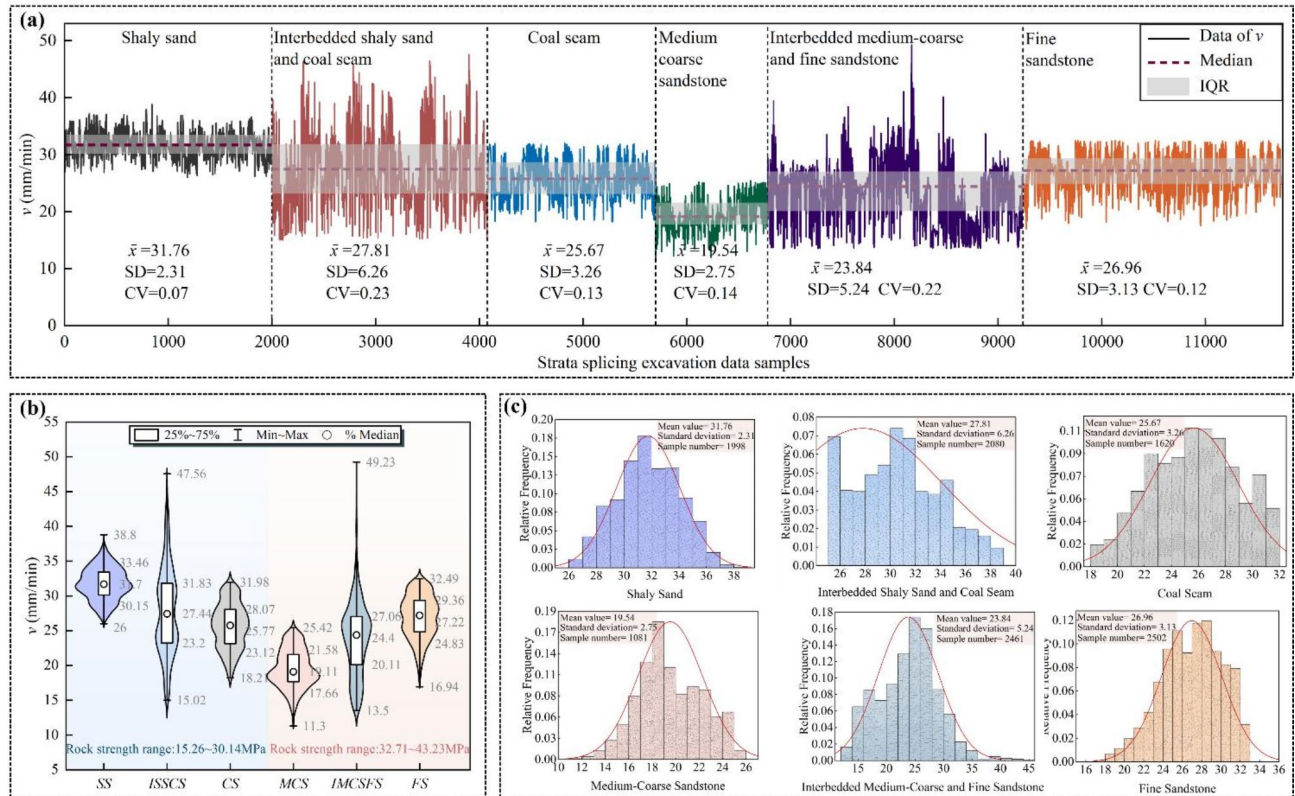


**Fig. 6.** Changing law of TBM tunneling speed parameters. (a) Line graph of tunneling speed in different strata; (b) Violin graph of tunneling speed in different strata; (c) Histogram of tunneling speed frequency in different strata.

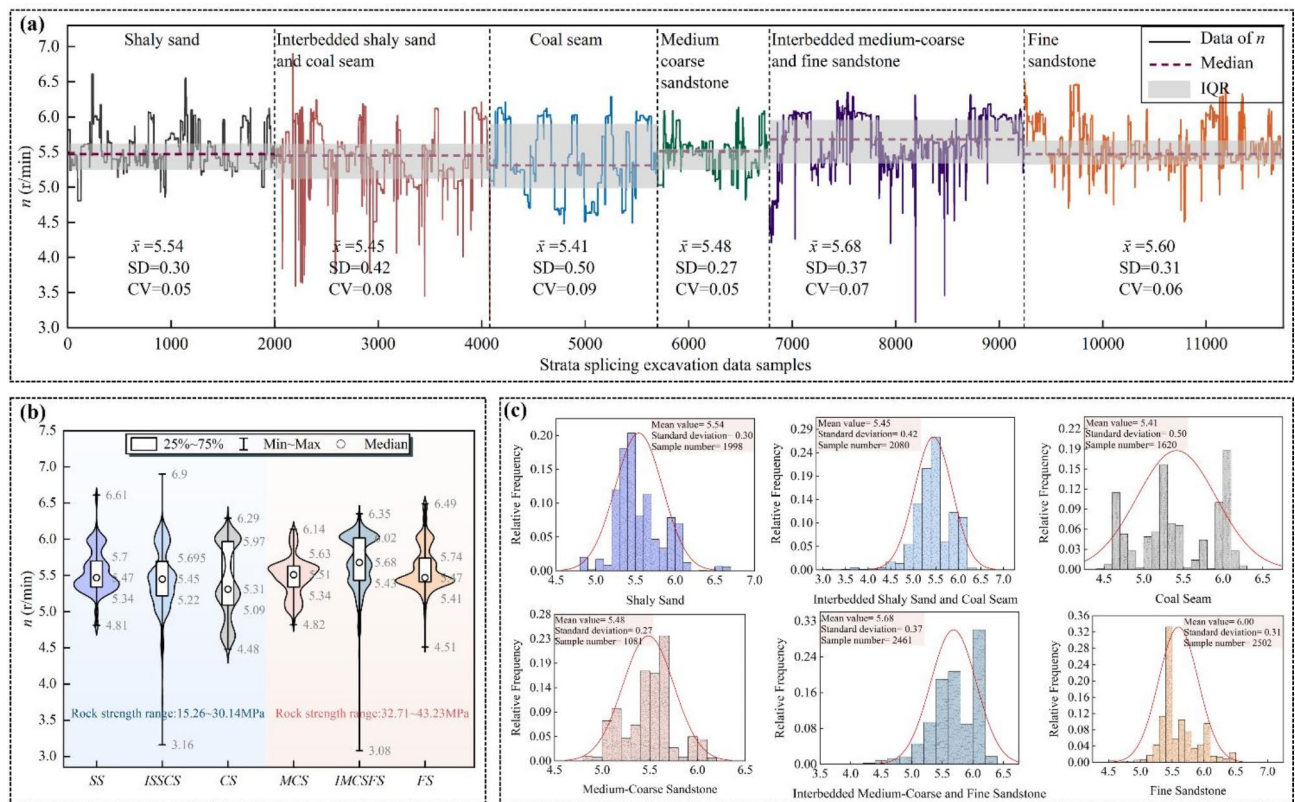


**Fig. 7.** Changing law of TBM cutter speed parameters. (a) Line graph of cutter speed in different strata; (b) Violin graph of cutter speed in different strata; (c) Histogram of cutter speed frequency in different strata.

As shown in Fig. 7b, c, the cutterhead speed under different strata conforms to the normal distribution. Except for multiple concentrated distributions in the coal seam, the remaining strata belong to a single distribution, and the quartile ranges are 5.34 ~ 5.70, 5.22 ~ 5.70, 5.09 ~ 5.97, 5.34 ~ 5.63, 5.43 ~ 6.02  $\text{r} \cdot \text{min}^{-1}$  and 5.41 ~ 5.74  $\text{r} \cdot \text{min}^{-1}$ , respectively. The rotation speed of the cutterhead under different strata is fine sandstone and medium-coarse sandstone interbedded > medium-coarse sandstone strata > fine sandstone strata > shaly sandstone strata > shaly sandstone and coal seam interbedded > coal seam, and its variation law is opposite to the tunneling speed. Because of the high strength of hard rock formation, the cutter resistance is large when the disc cutter breaks rock, and the larger cutter speed is helpful to improve the rock breaking efficiency. The weak stratum is evenly distributed, and a small rotation speed can achieve a good tunneling effect. If the rotation speed is too large, there will be a safety problem. However, the change of cutterhead speed in different strata is small, which is basically maintained at 5 ~ 6  $\text{r} \cdot \text{min}^{-1}$ , and its control range is small.

## Variation law of TBM passive performance parameters

### Cutter thrust

Cutter thrust is the forward force exerted by the cutter on the rock mass during tunneling and is usually measured in kilonewtons (kN). Cutter thrust can be measured by a pressure sensor mounted on the propulsion cylinder. The sensor detects the pressure in the cylinder and converts it into a thrust value. The changing law of the cutter thrust parameter in different lithologies and their composite strata is shown in Fig. 8. As shown in Fig. 8a, there is a significant difference in the cutter thrust force during the boring process in different types of rock strata. The amplitude of the tunneling data in muddy sandstone, coal bed and fine sandstone is small, and the coefficient of variation is 0.10 ~ 0.18; in the composite strata, the amplitude of the tunneling data increases, and the coefficient of variation is 0.24 ~ 0.27.

As shown in Fig. 8b, c, the total thrust under different strata conforms to the normal distribution. Except for multiple concentrated distributions in the medium-coarse sandstone strata, the remaining strata belong to a single distribution. The quartile ranges are 5504.22 ~ 6298.76, 3253.32 ~ 4308.41, 3037.48 ~ 3767.18, 5560.33 ~ 8230.96, 6242.28 ~ 8491.20 kN and 6517.88 ~ 8123.17 kN, respectively. The total thrust under different strata is: fine sandstone strata > medium-coarse sandstone strata > fine sandstone and medium-coarse sandstone interbedded > shaly sandstone strata > shaly sandstone and coal seam interbedded > coal seam. Compared with the hard stratum, the total thrust required for the relatively weak stratum is only half of the latter. Because the strength of the weak stratum is low, a higher tunneling speed can be obtained under a relatively small thrust. The strength of the hard stratum is large, and the total thrust required is also increased, but the tunneling speed is not high. Therefore, excessive total thrust is easy to cause the increase of tool resistance, accelerate tool wear and

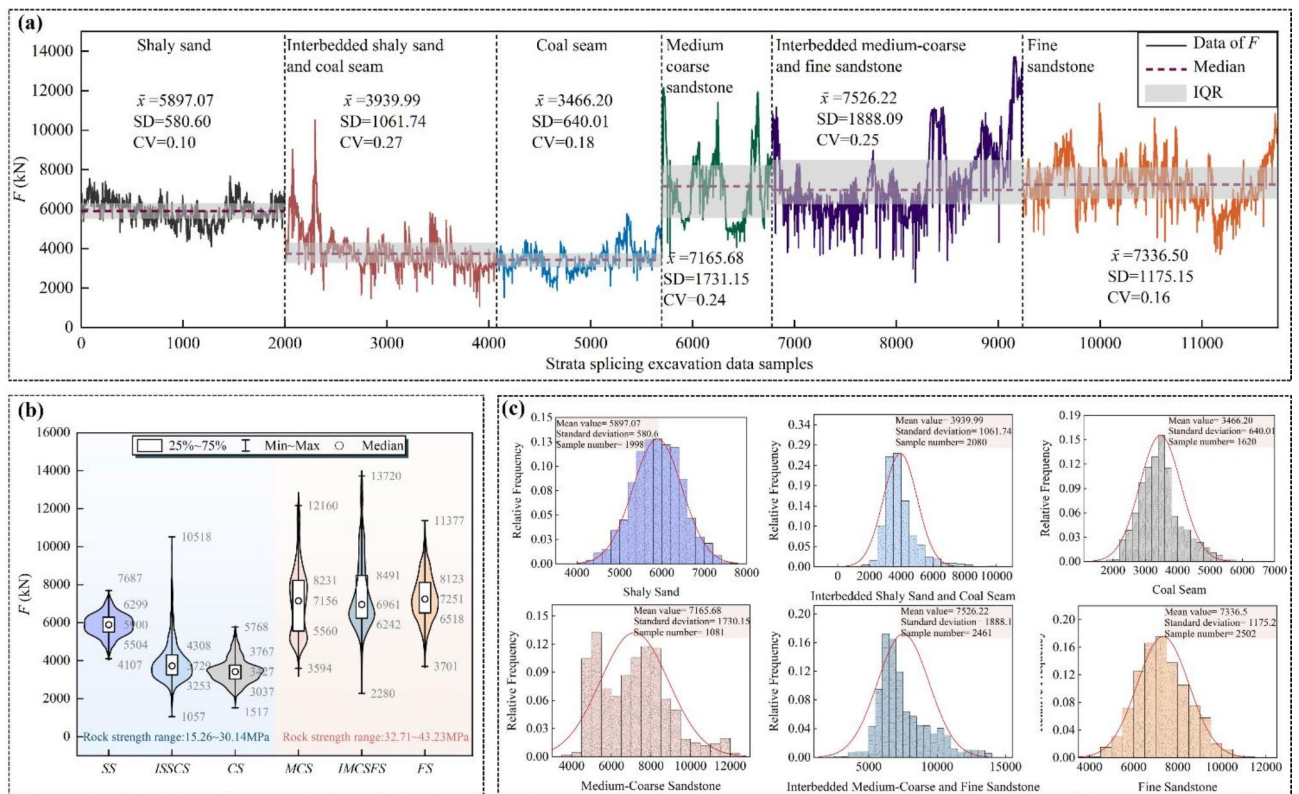


**Fig. 8.** Changing law of TBM cutter thrust parameters. (a) Line graph of cutter thrust in different strata; (b) Violin graph of cutter thrust in different strata; (c) Histogram of cutter thrust frequency in different strata.

reduce tool rock breaking ability. The recommended total thrust control ranges of the six lithologic strata are: 6518 ~ 8123 kN, 5560 ~ 8231 kN, 6242 ~ 8491 kN, 5504 ~ 6299 kN, 3253 ~ 4308 kN, 3037 ~ 3767 kN.

#### Cutterhead torque

Cutter torque is the rotational moment in kilonewton-meters (kN·m) that the cutter exerts on the rock during rotation. Cutter torque can be measured by a torque sensor. The sensor is mounted on the drive shaft of the cutterhead and detects the torque generated when the cutterhead rotates. The changing law of the cutter disk torque parameter in different lithologies and their composite formations is shown in Fig. 9. As shown in Fig. 9a, there is a significant difference in the cutterhead torque during the boring process in different types of rock strata. The coefficient of variation of the excavation data in the composite formation of muddy sandstone and coal seam reaches 0.52, and the data oscillate violently.

As shown in Fig. 9b, c, the cutterhead torque under different strata conforms to the normal distribution. Except for multiple concentrated distributions in fine sandstone strata, the remaining strata belong to a single distribution. The quartile ranges are 627.40 ~ 719.90, 124.51 ~ 233.10, 100.63 ~ 125.28, 624.64 ~ 876.30, 642.80 ~ 880.90 kN·m and 606.33 ~ 934.47 kN·m, respectively. The cutterhead torque under different strata is: fine sandstone and medium-coarse sandstone interbedded > fine sandstone strata > medium-coarse sandstone strata > shaly sandstone strata > shaly sandstone and coal seam interbedded > coal seam, and its variation law is consistent with the total thrust. The torque of the shaly sandstone and the coal seam is similar, and the average value is 195.15 kN·m and 117.17 kN·m. The cutterhead torque of the remaining rock strata is between 670 ~ 770 kN·m, which is about 4 ~ 6 times that of the weak rock strata, mainly because the hard rock strata need to overcome greater resistance and need greater torque. Therefore, the recommended cutterhead torque control range is 100 ~ 233 kN·m in soft strata and 606 ~ 934 kN·m in hard strata.

#### Variation law of TBM target parameters

In TBM boring parameters, penetration refers to the distance advanced by the cutter disk per revolution, usually in millimeters per revolution ( $\text{mm} \cdot \text{r}^{-1}$ ). It is an important index to measure the ability of the cutterhead to penetrate the rock during rotation, and is used to assess the efficiency of the cutterhead's penetration into the rock. The relationship between penetration and the speed of advancement and the rotational speed of the cutter can be expressed as follows:

$$P = \frac{v}{n} \quad (9)$$

where  $P$  is the penetration,  $\text{mm} \cdot \text{r}^{-1}$ ;  $v$  is the tunneling speed,  $\text{mm} \cdot \text{min}^{-1}$ ;  $n$  is the cutter speed,  $\text{r} \cdot \text{min}^{-1}$ .



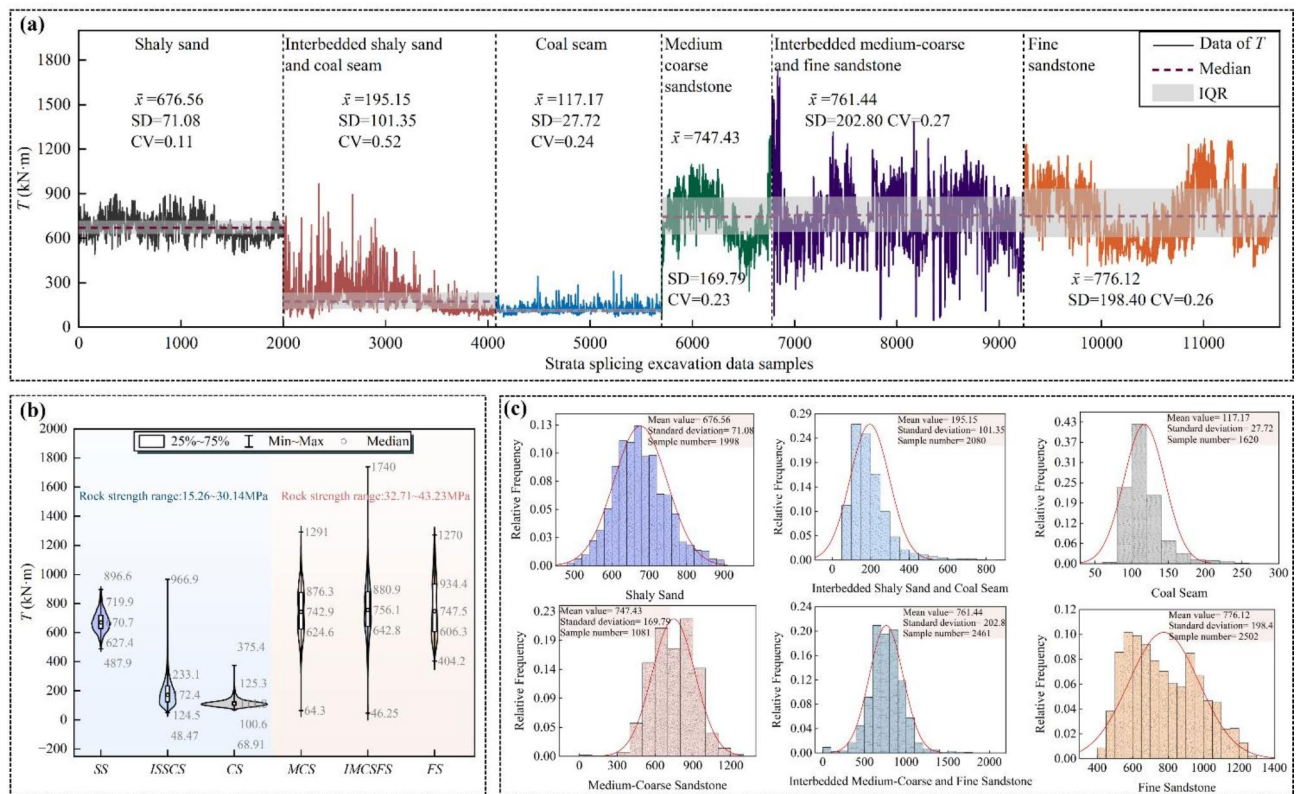


**Fig. 9.** Changing law of TBM cutter torque parameters. (a) Line graph of cutter torque in different strata; (b) Violin graph of cutter torque in different strata; (c) Histogram of cutter torque frequency in different strata.

The change rule of the penetration parameter in different lithologies and their composite strata is shown in Fig. 10. As shown in Fig. 10a, there are significant differences in the penetration degree of different types of rock strata in the boring process. Except for the large fluctuation of the penetration parameter in the composite stratum, it basically fluctuates around the average value in a single rock stratum, and the penetration of the muddy sandstone stratum has the smallest discrete type and is the most stable.

As shown in Fig. 10b, c, the penetration under different strata conforms to the normal distribution, and the distribution is uniform and stable. The quartile ranges are 5.3 ~ 6.1, 4.2 ~ 5.9, 4.2 ~ 5.2, 3.2 ~ 3.9, 3.5 ~ 4.7 mm·r<sup>-1</sup> and 4.2 ~ 5.2 mm·r<sup>-1</sup>, respectively. The cutterhead torque under different strata is: shaly sandstone stratum > shaly sandstone and coal seam interbedded > fine sandstone stratum > coal seam > fine sandstone and medium coarse sandstone interbedded > medium coarse sandstone stratum, and its variation law is consistent with the tunneling speed. The weak stratum is evenly distributed and can be well penetrated; the penetration of hard rock strata is small, mainly because the medium-coarse sandstone is relatively hard and has high strength, and the resistance of disc cutter rock breaking tool is large, so it is difficult to penetrate well. From the overall distribution of penetration in different strata in Fig. 10b, it can be seen that the average and median penetration of interbedded layers are always between adjacent two strata, and the distribution range of penetration is always greater than the extreme value range of penetration of two adjacent strata due to the existence of interbedded layers. Because of the change of the proportion of interbedded layers, the cutter head is more likely to deflect under different lithologic strength. Therefore, it is necessary to adapt to more complex working conditions. In summary, the relatively weak strata and the interbedded strata in the hard strata have the same change rule, and the data distribution is complicated and mainly concentrated in the middle of the adjacent two strata data.

### Analysis of TBM boreability in different lithology strata

The main parameters of TBM include active control parameters (cutterhead speed  $n$  and tunneling speed  $v$ ), passive performance parameters (cutter thrust  $F$  and cutterhead torque  $T$ ) and target parameters (penetration  $P$ ). However, these directly obtained parameters cannot directly reflect the tunneling efficiency of TBM in different strata. Through the above tunneling parameters, two derivative parameters of thrust factor  $F'$  and tunneling specific energy  $E_s$  can be obtained. Combining the characteristics of various parameters, the tunneling performance of TBM can be well reflected<sup>32</sup>.

### Thrust factor

The thrust factor is used to evaluate the propulsion efficiency of TBM in different geological conditions. In hard rock formations, the propulsive force is usually higher and the tunneling speed is slower, so the thrust factor is higher. On the contrary, in soft soil layer, the propulsion force is smaller, the tunneling speed is faster,

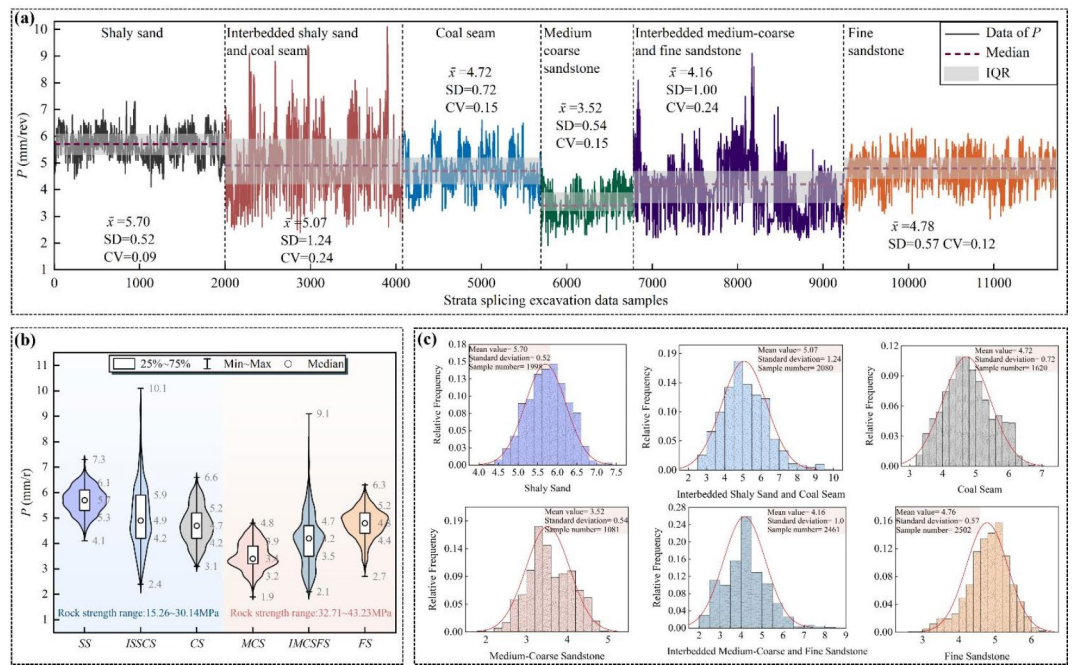


**Fig. 10.** Changing rules of TBM penetration parameters. (a) Line graph of penetration in different strata; (b) Violin graph of penetration in different strata; (c) Histogram of penetration frequency in different strata.

and the thrust factor is lower. The thrust factor represents the total thrust required per unit penetration, that is, the correlation between the magnitude of the TBM thrust and the strength of the surrounding rock, reflecting the drivability of the formation<sup>33</sup>, which is defined as shown in Eq. (10). In the process of TBM tunneling, the penetration is affected by the tunneling speed and the cutterhead speed, which is defined as the distance of each rotation of the cutterhead, which can directly reflect the tunneling efficiency. In the case of other tunneling parameters unchanged, the penetration decreases with the increase of surrounding rock strength. Under the same formation conditions, the penetration increases with the increase of the total thrust, so the thrust factor is introduced, and the time domain diagram is shown in Fig. 11.

$$F' = \frac{F}{P} \quad (10)$$

Among them  $F'$  ( $\text{kN} \cdot \text{r} \cdot \text{mm}^{-1}$ ) is the propulsion factor,  $F$  ( $\text{kN}$ ) and  $P$  ( $\text{mm} \cdot \text{r}^{-1}$ ) are the total thrust and penetration of TBM, respectively.

The variation trend of TBM thrust factor in different strata is shown in Fig. 11a. Under different formation conditions, the propulsion factor varies with the tunneling mileage, and increases with the increase of formation lithology strength. The thrust factor of shaly sandstone layer ranges from 692 to 1548  $\text{kN} \cdot \text{r} \cdot \text{mm}^{-1}$ , with an average of 1042  $\text{kN} \cdot \text{r} \cdot \text{mm}^{-1}$ . The thrust factor of shaly sandstone and coal seam composite formation ranges from 252  $\text{kN} \cdot \text{r} \cdot \text{mm}^{-1}$  to 3364  $\text{kN} \cdot \text{r} \cdot \text{mm}^{-1}$ , with an average of 832  $\text{kN} \cdot \text{r} \cdot \text{mm}^{-1}$ . The thrust factor in the medium-coarse sandstone layer varies from 1088  $\text{kN} \cdot \text{r} \cdot \text{mm}^{-1}$  to 4493  $\text{kN} \cdot \text{r} \cdot \text{mm}^{-1}$ , with an average of 2070  $\text{kN} \cdot \text{r} \cdot \text{mm}^{-1}$ . The thrust factor in the composite formation of medium coarse sandstone and fine sandstone varies from 675  $\text{kN} \cdot \text{r} \cdot \text{mm}^{-1}$  to 5449  $\text{kN} \cdot \text{r} \cdot \text{mm}^{-1}$ , with an average of 1935  $\text{kN} \cdot \text{r} \cdot \text{mm}^{-1}$ . The thrust factor in the fine sandstone layer ranges from 832 to 2889  $\text{kN} \cdot \text{r} \cdot \text{mm}^{-1}$ , with an average of 1555  $\text{kN} \cdot \text{r} \cdot \text{mm}^{-1}$ . Compared with the single formation, the variation amplitude of the propulsion factor in the composite formation is larger, which is 1.50 ~ 3.64 times that of the latter.

The relationship between TBM propulsion factor and penetration in different strata is shown in Fig. 11b. According to the definition of thrust factor, it is negatively correlated with penetration. However, under different formation conditions, with the increase of penetration, the fluctuation of thrust factor decreases significantly, that is, the greater the penetration, the more concentrated the thrust factor. The linear fitting of propulsion factor and penetration degree under different formation conditions is carried out. In relatively weak strata, the correlation coefficient of composite strata is much smaller than that of adjacent single strata. In hard rock strata, the fitting correlation coefficient is opposite.

### Energy parameters

The tunneling efficiency is affected by various factors, such as driving loads, geological conditions and operating conditions. In TBM boring process, TBM is driven by thrust and torque. Under the condition that other tunneling parameters remain unchanged, the increase of cutter torque and cutter thrust will consume more



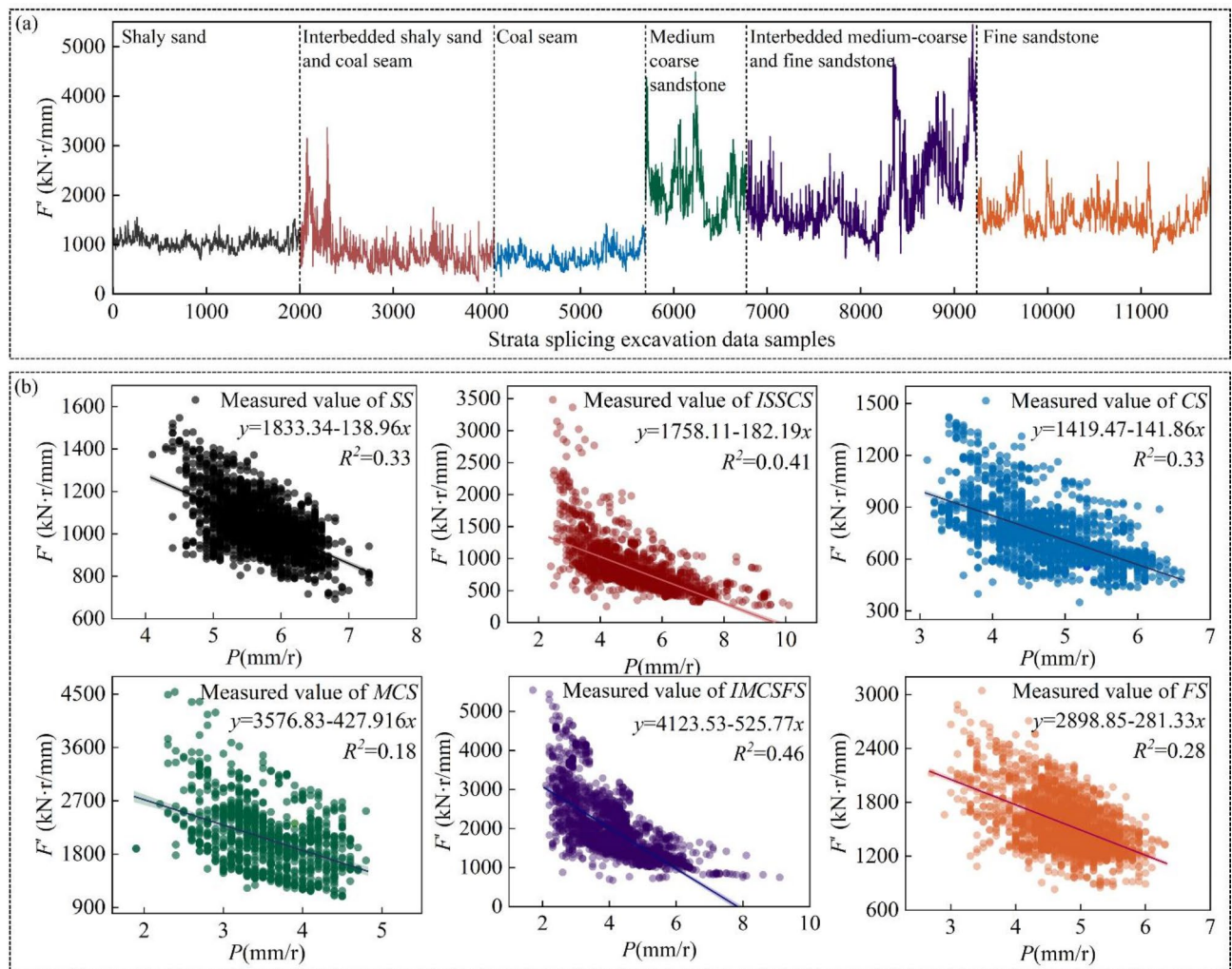


**Fig. 11.** The variation law of thrust factor. (a) Time domain diagram of thrust factor in different strata; (b) The relationship between thrust factor and penetration in different strata)

tunneling energy. Excavation specific energy ( $E_s$ ) indicates the energy consumption of TBM for excavating a unit volume of rock and soil, and the excavation specific energy is a key index to measure the efficiency of TBM excavation<sup>34</sup>. In hard rock formations, the hardness of the rock is higher, and more energy is needed to break the rock, so the tunneling specific energy is larger. In soft rock formations, the hardness of the rock is lower, less energy is needed, and the tunneling specific energy is smaller. Defined as:

$$E_s = \frac{Fv + 2\pi Tn}{\pi R^2 v} \quad (11)$$

Among them,  $E_s$  ( $\text{J} \cdot \text{m}^{-3}$ ) is the tunneling specific energy,  $v$  ( $\text{mm} \cdot \text{min}^{-1}$ ) is the tunneling speed,  $T$  ( $\text{kN} \cdot \text{m}$ ) is the cutterhead torque,  $n$  ( $\text{r} \cdot \text{min}^{-1}$ ) is the cutterhead speed, and  $R$  (m) is the cutterhead radius.

As shown in Eq. (11), the tunneling specific energy mainly depends on the driving load and the penetration depth per revolution. The load is affected by geological conditions and operating conditions. Due to the complex interaction between the cutterhead and the stratum during the tunneling process, the change of this parameter has a strong correlation with the change of rock strength<sup>35</sup>, and the time domain diagram is shown in Fig. 12.

The variation trend of the specific energy of TBM in the process of tunneling in different strata is shown in Fig. 12a. It can be seen from the figure that in the relatively weak rock strata, the change trend of tunneling specific energy is relatively stable, and the tunneling specific energy gradually decreases from the whole section of shaly sandstone layer to the whole section of coal seam. In the hard rock stratum, the change trend of tunneling specific energy has strong oscillation, but the whole tends to the same level. The statistical results show that the tunneling specific energy of shaly sandstone layer varies from  $161 \text{ J} \cdot \text{m}^{-3}$  to  $266 \text{ J} \cdot \text{m}^{-3}$ , with an average of  $211 \text{ J} \cdot \text{m}^{-3}$ . The specific energy of shaly sandstone and coal seam composite strata ranges from 36 to  $340 \text{ J} \cdot \text{m}^{-3}$ , with an average of  $133 \text{ J} \cdot \text{m}^{-3}$ . The tunneling specific energy of coal seam ranges from  $53 \text{ J} \cdot \text{m}^{-3}$  to  $188 \text{ J} \cdot \text{m}^{-3}$ , with an average of  $115 \text{ J} \cdot \text{m}^{-3}$ . The excavation specific energy in the medium-coarse sandstone layer ranges from 121 to  $417 \text{ J} \cdot \text{m}^{-3}$ , with an average of  $271 \text{ J} \cdot \text{m}^{-3}$ . The specific energy of tunneling in the composite

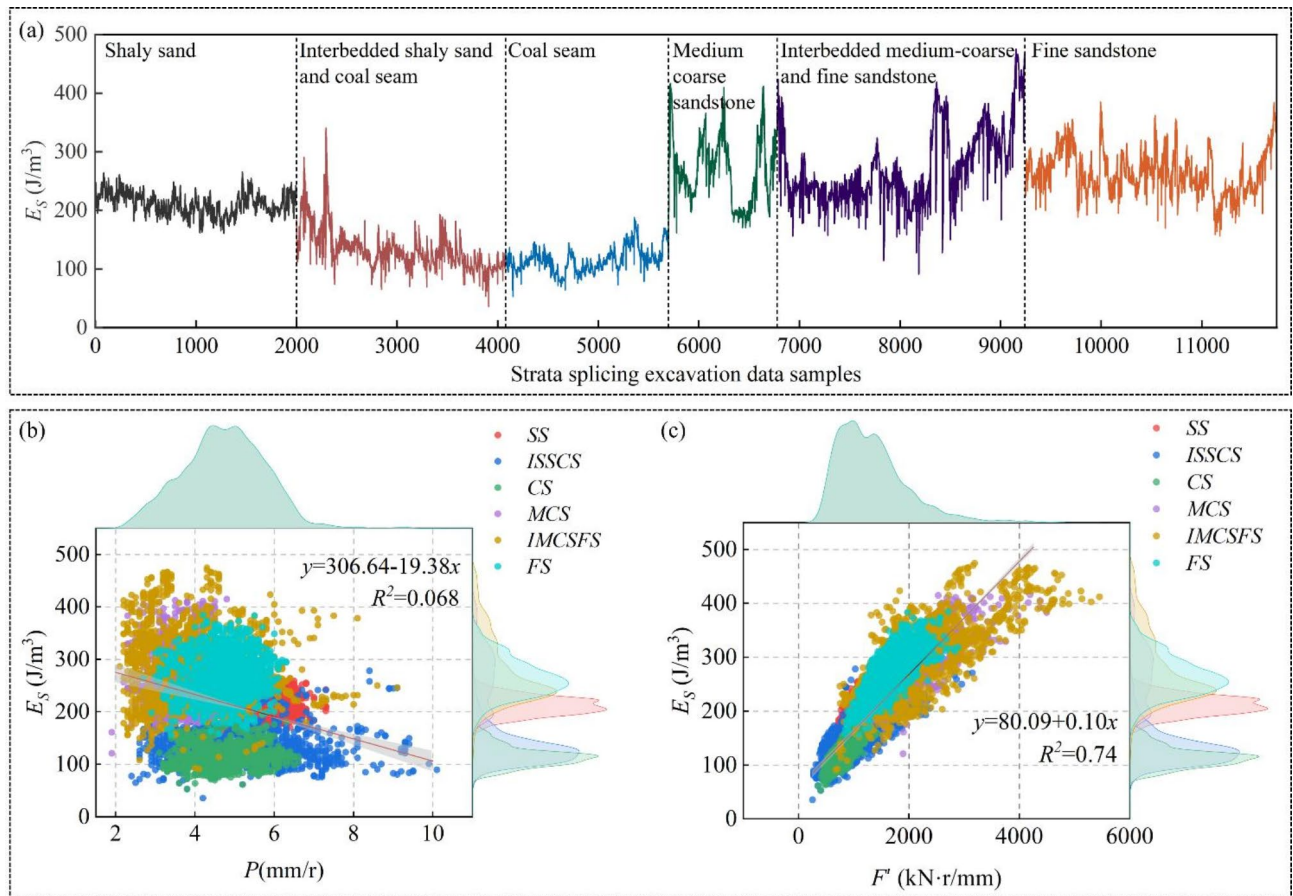


**Fig. 12.** The variation law of tunneling specific energy. (a) Time domain diagram of tunneling specific energy in different strata; (b) The relationship between tunneling specific energy and penetration, thrust factor in different strata)

formation of medium coarse sandstone and fine sandstone varies from  $91 \text{ J} \cdot \text{m}^{-3}$  to  $474 \text{ J} \cdot \text{m}^{-3}$ , with an average of  $277 \text{ J} \cdot \text{m}^{-3}$ . The thrust factor in the fine sand layer ranges from  $156$  to  $385 \text{ J} \cdot \text{m}^{-3}$ , with an average of  $266 \text{ J} \cdot \text{m}^{-3}$ . Compared with the single stratum, the oscillation amplitude of the tunneling specific energy change in the composite stratum is larger, which is  $1.29 \sim 2.25$  times that of the latter.

The relationship between tunneling specific energy and penetration is shown in Fig. 12b. The relationship between specific energy and propulsion factor is shown in Fig. 12c. It can be seen from the figure that the tunneling specific energy is negatively correlated with the penetration degree and positively correlated with the propulsion factor. Based on the linear fitting analysis of TBM tunneling specific energy, penetration degree and propulsion factor under 6 stratum conditions, it can be seen that the correlation between tunneling specific energy and penetration degree is not obvious, and the correlation coefficient is only 0.068. The fitting coefficient with the propulsion factor can reach 0.74, indicating that the correlation between the tunneling specific energy and the propulsion factor is significant. With the increase of the propulsion factor, the tunneling specific energy also increases linearly. By analyzing the marginal distribution of tunneling specific energy in different strata, it can be seen that the tunneling specific energy in the composite strata of medium-coarse sandstone and fine sandstone has the largest discreteness, which is medium-coarse sandstone layer, fine sandstone layer, shaly sandstone and coal seam composite stratum, coal seam and shaly sandstone layer.

### Classification of stratum excavation difficulty

Strata drivability refers to the matching degree between the actual performance of TBM and the tunneling target in the case of continuous tunneling in different strata. Among them, the fast tunneling speed and low energy consumption during TBM tunneling are taken as the tunneling target. The characteristic parameters cannot be obtained directly, and can only be characterized by the state law of tunneling behavior in different strata. Among them, the parameters describing tunneling behavior are tunneling speed and tunneling specific energy. In order to eliminate the problem that the tunneling parameters generated by the equipment in different strata cannot be effectively compared, the two indicators are normalized to obtain dimensionless parameters. The energy efficiency index (Tunneling speed index  $VI$ , Tunneling energy consumption index  $E_s I$ ) of TBM tunneling in different strata is defined as<sup>36</sup>:

$$VI_i = \frac{v_i - \min(v)}{\max(v) - \min(v)} \quad (12)$$

$$E_{SI_i} = \frac{E_{S_i} - \min(E_S)}{\max(E_S) - \min(E_S)} \quad (13)$$

The boreability of the stratum is divided into four grades (I, II, III, IV), and each of the characterization indexes (tunneling speed index  $VI$ , tunneling energy consumption index  $E_{SI}$ ) is divided into 9 grades ( $L_1 \sim L_9$ ), and the indexes of each grade are classified. With the gradual increase of the serial number of the grade, the tunneling speed and the tunneling energy consumption decrease in turn, and the boreability becomes worse. Therefore, the level of tunneling speed index  $VI$  is labeled inversely, which is consistent with the change trend of tunneling energy consumption index. According to the expression of the tunneling speed index of Eq. (12) and the tunneling energy consumption index of Eq. (13), the values are normalized to the interval of [0, 9], and the histograms of frequency distribution of the two indices in each stratum are plotted as shown in Fig. 13, which indicates the distribution law of the sample characteristics of each stratum.

The characteristic data intervals of the horizontal axis intervals ( $\bar{x} - \sigma$ ,  $\bar{x} + \sigma$ ) formed by the mean value  $\bar{x}$  and  $1\sigma$  standard deviation  $\sigma$  under the normal distribution curves corresponded to the level ranges of the tunneling effectiveness characteristics of the ground palisade, and the means and standard deviations of the two tunneling effectiveness characteristics are shown in Table 3.

In order to reduce the influence of feature data spanning on feature parameter levels, the average value of the feature level range of tunneling energy efficiency in each stratum is used, multiplied by a feature level range correction factor  $k$ .  $k$  denotes the parameter level correction factor for each stratum feature from, i.e., the maximum value of the number of levels spanned by the histogram of feature parameters in the current stratum divided by the number of levels spanned in each stratum. This is shown in Eq. (14).

$$\begin{cases} L_i = \frac{\min(L_i) + \max(L_i)}{2} \cdot k \\ k = \frac{k_j}{\max k_j}, k_j = [\max(L_i) - \min(L_i) + 1] \end{cases} \quad (14)$$

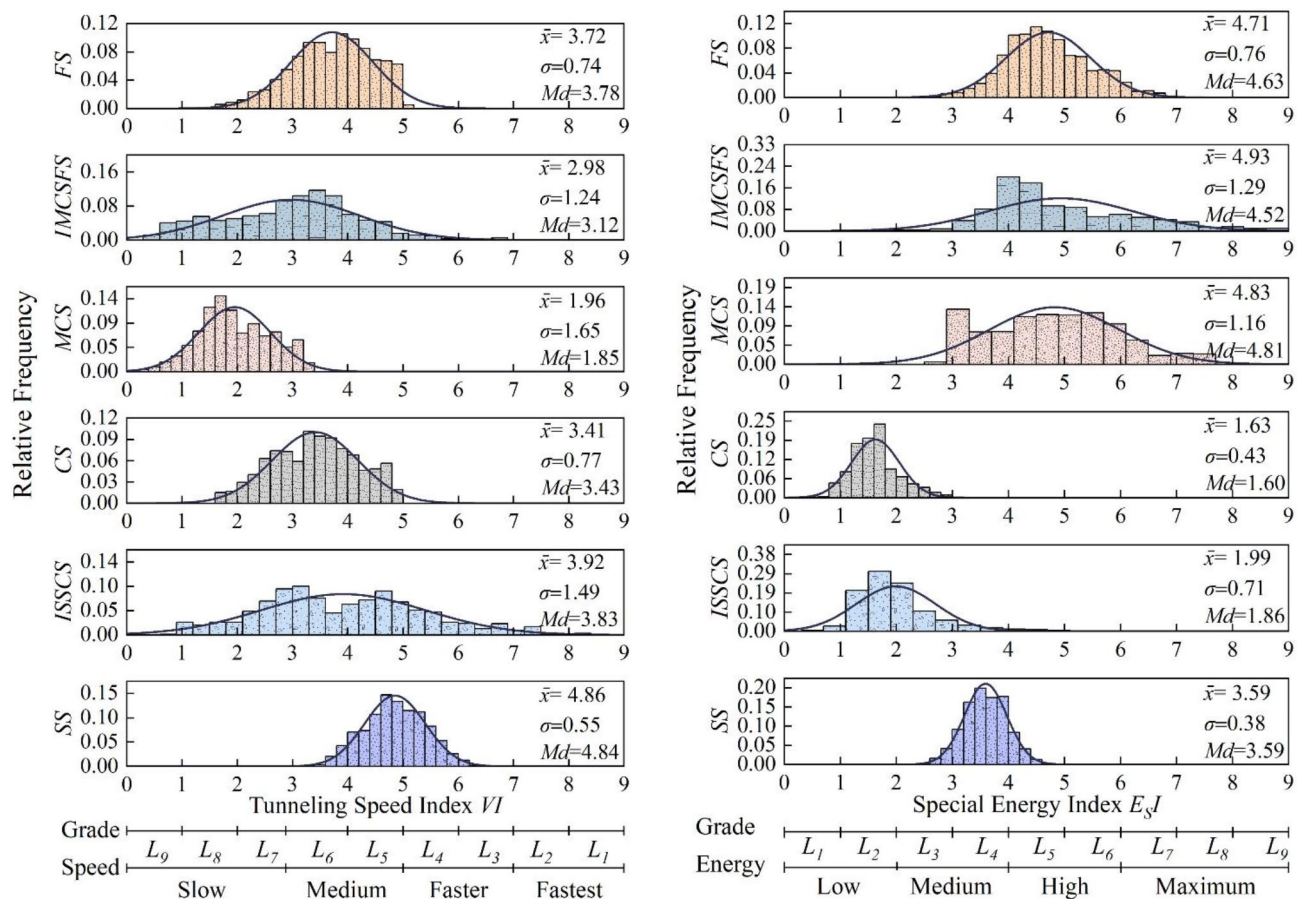


**Fig. 13.** Characteristic frequency distribution histogram and level division of tunneling efficiency in each stratum.



Strata classification indicators		Strata information					
		SS	ISSCS	CS	MCS	IMCSFS	FS
VI	Average values	4.86	3.92	3.41	1.96	2.98	3.72
	Standard deviation	0.55	1.49	0.77	1.65	1.24	0.74
$E_sI$	Average values	3.59	1.99	1.63	4.83	4.93	4.71
	Standard deviation	0.38	0.71	0.43	1.16	1.29	0.76

**Table 3.** Means and standard deviations of stratigraphic classification indicators for various types of strata.

Strata classification indicators	Levels of difficulty	Special energy index $E_sI$			
		1 ~ 2	3 ~ 4	5 ~ 6	7 ~ 9
Tunneling speed index VI	1 ~ 2	I	I	II	III
	3 ~ 4	I	II	III	III
	5 ~ 6	II	III	III	IV
	7 ~ 9	III	III	IV	IV

**Table 4.** Tunneling energy efficiency ratings for combinations of indicators.

Stratum	VI			$E_sI$			Boreability Grade
	Rank range	Correction factor	Level	Rank range	Correction factor	Level	
SS	$L_4 \sim L_5$	0.50	$L_3$	$L_4 \sim L_4$	0.25	$L_1$	I
ISSCS	$L_4 \sim L_7$	1.00	$L_6$	$L_2 \sim L_3$	0.50	$L_2$	II
CS	$L_5 \sim L_7$	0.75	$L_5$	$L_2 \sim L_2$	0.25	$L_1$	II
MCS	$L_6 \sim L_9$	1.00	$L_8$	$L_4 \sim L_6$	0.75	$L_4$	III
IMCSFS	$L_5 \sim L_8$	1.00	$L_7$	$L_4 \sim L_7$	1.00	$L_6$	IV
FS	$L_5 \sim L_6$	0.50	$L_3$	$L_5 \sim L_6$	0.5	$L_3$	II

**Table 5.** The classification of ground drivability based on TBM tunneling parameters.

Among them,  $L_i$  (value 1 ~ 9) represents the level value of the characteristic parameters,  $k_j$  represents the influence factor of the level range of the corresponding formation characteristic parameters, and  $j$  value is 1 ~ 6.

The corrected level values of the two tunneling efficiency characteristics can be obtained from Eq. (14). According to the corrected level values, the efficiency level of TBM tunneling in different strata can be obtained by referring to Table 4. Grade I indicates the best tunneling performance, grade II indicates better tunneling performance, grade III indicates average tunneling performance, and grade IV indicates the worst tunneling performance. Through the calculation, the value of TBM’s boreability grade and its grading in all kinds of strata are shown in Table 5.

As can be seen from Table 5, during the tunneling process of 1# back-air alley in the west area, TBM has the best performance in muddy sandstone layer, with the highest boreability; the performance in muddy sandstone and coal seam interbed, coal seam and fine sandstone is the second best, with better boreability; the performance in medium-coarse sandstone layer is general, with average boreability; the performance in medium-coarse sandstone and fine sandstone layer is the worst, and the boreability is more difficult. From the point of view of the tunneling situation of single stratum and composite stratum, the boreability of composite stratum is always 1 ~ 2 grades lower than that of the adjacent single stratum.

Discussion

In composite strata, the fluctuation of TBM tunneling parameters has a significant impact on the tunneling efficiency. How to optimize and regulate the TBM tunneling parameters by using the massive tunneling data collected in the process of TBM tunneling, and timely and effectively guide the TBM tunneling efficiency in the complex geological situation, is a field engineering problem that we have been trying to solve. Combining the lithology of each stratum and the adaptability of TBM tunneling, the paper gives the tunneling parameter regulation range in line with the actual situation of each lithology, in order to adapt to different geological conditions, so as to optimize the tunneling efficiency. At the same time, based on the tunneling speed index and tunneling energy consumption index, the formation boreability class identification method is established, and the characteristic parameter fluctuation correction factor is proposed to quantitatively evaluate the degree of tunneling difficulty in six types of formations. The proposed stratum boreability class identification method can effectively classify the composite strata, and provide important reference and guidance for the assessment and prediction of TBM boreability in different strata and the optimization and control of tunneling parameters<sup>37</sup>.

While current research has provided valuable insights into TBM tunnelability in composite formations, there are still many areas of future research directions to be explored. The following are some of the potential research directions:

**Dynamic monitoring of geologic conditions:** Currently, TBM tunneling mainly relies on in-situ testing and core testing to obtain the main parameters of the rock mass, but these methods are difficult to dynamically sense the changes in the main mechanical parameters of the rock mass. Future research can explore how to utilize real-time monitoring technology, such as geostatistical methods and machine learning algorithms, to dynamically predict and be informed of the mechanical parameters of the rock body in front, so as to timely adjust the TBM tunneling parameters, improve the efficiency of the tunneling, and reduce the abnormal wear.

**Combined rock-breaking technology:** With the implementation of China's "One Belt, One Road", CZ Railway, Yangtze River Economic Belt and other national strategies, the demand for TBM is increasing. The traditional TBM's mechanical tool rock breaking mode has reached a bottleneck, future research can explore the traditional cutter tool mechanical rock breaking and hydraulic, laser and other technologies to form a joint rock breaking method, to realize the innovation of TBM's rock breaking method and improve the efficiency of tunneling.

**Intelligent and automation technology:** The application of modern technology in TBM is becoming more and more extensive, future research can further explore how to use intelligent and automation technology, such as convolutional neural network (CNN) and bidirectional gated recurrent unit (BiGRU) neural network, to build a more accurate prediction model of tunneling parameters, and to improve the efficiency and safety of the TBM tunneling.

**Over-advanced geological forecasting technology:** In TBM construction, over-advanced geological forecasting technology is an important means to cope with extreme complex geology. Future research can explore how to improve the accuracy of the over-advanced geological forecasting technology, especially in the quantitative prediction of the geological conditions in the middle and long distances.

**Adaptability in composite strata:** The adaptability of TBMs in composite strata is an important issue. Future research can further explore how to optimize the design and operation parameters of TBM to improve its boring efficiency and safety in composite formations.

**Improvement of formation boreability evaluation standard:** The current evaluation of formation boreability mainly relies on the tunneling speed and tunneling energy consumption indexes, and future research can explore more comprehensive evaluation indexes, such as the results of geological over-forecasting, physical and mechanical properties of rock body, etc., in order to more comprehensively assess the boreability of the formation. A real-time feedback mechanism is established to dynamically adjust the evaluation criteria of formation boreability according to the actual data in the process of tunneling, so as to improve the accuracy and practicability of the evaluation.

Through these future research directions, the tunneling parameters of TBM in different geological conditions can be further optimized to improve the construction efficiency, reduce the construction cost, and ensure the construction safety. These researches not only contribute to the theoretical development, but also provide important references and guidance for actual projects.

## Conclusion

In order to explore the mapping relationship between TBM tunneling parameters and strata, this paper starts from the characteristics of tunneling parameters and derivative parameters, combined with the equipment parameters, tunneling parameters and geological parameters in the tunneling of 1# return air development roadway in the west area of a mine in Binchang, Shaanxi Province, and excavates the correlation between TBM tunneling parameters and between tunneling parameters and strata. The drivability evaluation of six typical coal measures strata is carried out from three aspects: TBM tunneling parameters, energy parameters and tunneling capacity parameters. The specific conclusions are as follows:

(1) By analyzing the parameters of TBM equipment, five main tunneling parameters are selected for parameter preprocessing and feature analysis. The effective parameters in stable tunneling state are obtained by using binary discrimination quartile method, histogram method and smoothing method. Pearson correlation coefficient is used to analyze the correlation between the single variables of tunneling parameters. The results show that the correlation coefficient between the penetration degree of target parameters and the tunneling speed of active control parameters is 0.98, which is extremely correlated, while the correlation between other parameters is quite different.

(2) The excavation parameters under different strata are basically normal distribution. According to the distribution law of tunneling parameters in shaly sandstone layer, shaly sandstone and coal seam interbedded layer, coal seam, fine sandstone layer, fine sandstone and medium coarse sandstone interbedded layer and medium coarse sandstone layer, the control range of tunneling speed, cutterhead speed, total thrust, cutterhead torque and penetration degree is optimized, and the reasonable control range is given respectively. It can provide a basis for decision-making control of TBM tunneling parameters in deep composite strata.

(3) When the TBM is tunneling from the full-face shaly sandstone layer to the full-face coal seam, the mean value of the propulsion factor and the tunneling specific energy gradually decreases, but the overall fluctuation range is relatively stable. When the whole section is excavated from the coarse sandstone layer to the fine sandstone layer of the whole section, the mean value of the propulsion factor and the tunneling specific energy does not change much, but the overall change trend has strong oscillation. At the same time, the oscillation amplitude of the composite formation is 1.29 ~ 3.64 times that of the single formation. According to the linear fitting results, the penetration degree is negatively correlated with the propulsion factor and the tunneling specific energy, and the tunneling specific energy is positively correlated with the propulsion factor, and the fitting coefficient is 0.74.

(4) Formation boreability evaluation indexes based on tunneling speed index and tunneling energy consumption index were established, and the frequency distribution histograms of the two indexes in each



formation were plotted, and the mean and standard deviation of the characteristic indexes were calculated to determine the corresponding grade ranges of the indexes. At the same time, the influence factor  $k$  of the level range of the characteristic parameters is proposed to eliminate the influence of the volatility of the characteristic parameters on the difficulty of tunneling. among the six strata, the muddy sandstone layer has the best boreability, which is class I; the muddy sandstone composite stratum with coal beds, the coal beds and the fine sandstone have better boreability, which is class II; the medium-coarse sandstone has general boreability, which is class III; and the medium-coarse sandstone composite stratum with fine sandstone has more difficult boreability, which is class IV.

## Data availability

The raw data of the study can be obtained from the corresponding author on enquiry.

Received: 2 September 2024; Accepted: 18 February 2025

Published online: 08 April 2025

## References

1. Fu, K. et al. Research on optimization strategy of TBM tunneling parameters based on stratum perception and simulation tunneling experiment. *Tunn. Undergr. Space Technol.* **147**, 105743 (2024).
2. Guo, X. et al. Equipment selection and adaptive design of rock drifting with TBM in deep coal mine. *Coal Eng.* **54** (05), 9–13 (2022).
3. Ding, Z. et al. Three-dimensional geological modeling technology based on PSO-Kriging algorithm. *Coal Eng.* **56** (10), 82–89 (2024).
4. Cai, J. et al. *The Application of Distributed Fiber-Optic Sensing Technology in Monitoring the Loose Zone in the Floor of Stopping Roadway* 1–22 (Rock Mechanics and Rock Engineering, 2024).
5. Ding, Z. et al. Study on the evolution law of bottom plate stress and reasonable roadway misalignment in downstream mining of coal seam group. *J. Xi'an Univ. Sci. Technol.* **44** (02), 213–225 (2024).
6. Wang, R. & Zhang, L. K-means-based heterogeneous tunneling data analysis method for evaluating rock mass parameters along a TBM tunnel. *Sci. Rep.* **13**, 21564 (2023).
7. Xue, Y. et al. An experimental study on mechanical properties and fracturing characteristics of granite under high-temperature heating and liquid nitrogen cooling Cyclic treatment. *Geoenergy Sci. Eng.* **237**, 212816 (2024).
8. Wang, M. & Wan, W. A new empirical formula for evaluating uniaxial compressive strength using the Schmidt hammer test. *Int. J. Rock Mech. Min. Sci.* **123**, 104094 (2019).
9. Wang, M., Wan, W. & Zhao, Y. Experimental study on crack propagation and coalescence of rock-like materials with two pre-existing fissures under biaxial compression. *Bull. Eng. Geol. Environ.* **79** (6), 3121–3144 (2020).
10. Wang, M. et al. Experimental and numerical study on peak strength, coalescence and failure of rock-like materials with two folded preexisting fissures. *Theoret. Appl. Fract. Mech.* **125**, 103830 (2023).
11. Wang, M., Wan, W. & Zhao, Y. Prediction of uniaxial compressive strength of rocks from simple index tests using random forest predictive model. *Comptes Rendus Mécanique.* **348** (1), 3–32 (2020).
12. Wang, M. et al. Calibrating microparameters of DEM models by using CEM, DE, EFO, MFO, SSO algorithms and the optimal hyperparameters. *Comput. Part. Mech.* **11**, 839–852 (2024).
13. Wang, M. et al. A calibration framework for the microparameters of the DEM model using the improved PSO algorithm. *Adv. Powder Technol.* **32**, 358–369 (2021).
14. Wang, Y. et al. Evolution patterns of tunneling parameters of Earth pressure balance shield in typical strata in Nanchang, China, and its stratigraphic boreability. *Tunn. Constr.* **43** (S2), 263 (2023).
15. Yang, T., Li, L. & Gong, J. Variation rule and correlation analysis of tunneling parameters of EPB-TBM dual-mode shield in composite stratum. *Constr. Technol.* **52** (13), 72–78 (2023).
16. He, C. et al. Research on the tunneling parameters and adaptability of EPB/TBM dual-mode shield in composite strata. *J. Railway Eng. Soc.* **40** (03), 96–103 (2023).
17. He, C. et al. Tunneling parameters and comparison of adaptability for compound strata of dual-mode shield machine. *Chin. J. Geotech. Eng.* **43** (01), 43–52 (2021).
18. Xia, Y. et al. Correlation analysis of TBM operating parameters and different lithologic strata. *J. Northeastern Univ. (Natural Science).* **42** (03), 401–407 (2021).
19. Zhao, B. et al. Variation of shield boring parameters and correlation analysis in mixed ground. *China Civil Eng. J.* **50** (S1), 140–144 (2017).
20. Huang, J. et al. Stratigraphic correlation of EFPI and evolution regularity of shield tunneling parameter in complex stratum. *Tunn. Constr.* **41** (S2), 215–221 (2021).
21. Duan, Z. et al. Relation of tunneling parameters of single shield TBM in sandstone and sandy Mud-stone stratum. *Urban Mass. Transit.* **22** (07), 120–125 (2019).
22. Wu, Z. et al. A classification and boreability perception and recognition method for rock mass based on TBM tunneling performance. *Chin. J. Rock Mechan. Eng.* **41** (S1), 2684–2699 (2022).
23. Wu, X. et al. Prediction and classification of rock mass boreability in TBM tunnel. *Rock. Soil. Mech.* **41** (05), 1721–1729 (2020).
24. Zhang, N. et al. Prediction method of Rockmass parameters based on tunnelling process of tunnel boring machine. *J. Zhejiang University(Engineering Science).* **53** (10), 1977–1985 (2019).
25. Qiao, G. Real-time identification method of stratum characteristics during shield tunnelling. *Chin. J. Undergr. Space Eng.* **19** (06), 2039–2044 (2023).
26. Zhang, X. et al. Research on surrounding rock feature identification method of coal mine roadway based on tunneling parameters. *Saf. Coal Mines.* **54** (12), 143–150 (2023).
27. Xie, Y. et al. A novel classification method of rock mass for TBM tunnel based on penetration performance. *Chin. J. Rock Mechan. Eng.* **37** (S1), 3382–3391 (2018).
28. Wu, F. et al. Development and application of Cutterhead vibration monitoring system for TBM tunnelling. *Int. J. Rock Mech. Min. Sci.* **146**, 104887 (2021).
29. Zhao, X. & Li, B. Application of outlier detection method in civil aviation alarm. *J. Nanjing Univ. Aeronaut. Astronaut.* **49** (4), 524–530 (2017).
30. Wang, S. et al. Study of standardized pre-processing method of TBM tunnelling data. *Mod. Tunn. Technol.* **59** (2), 38–44 (2022).
31. Marc, W. & Tucker, S. The trilemma between accuracy, timeliness and smoothness in real-time signal extraction. *Int. J. Forecast.* **37** (3), 1072 (2021).
32. Zhang, Y. et al. Correlative analysis of shield tunneling data and recognition of geologic features. *J. Harbin Eng. Univ.* **32** (4), 476–480 (2011).

33. Rohola, H. et al. Parametric study of the impacts of various geological and machine parameters on thrust force requirements for operating a single shield TBM in squeezing ground. *Tunneling Undergr. Space Technol.* **73** (1), 252–260 (2018).
34. Teale, R. The concept of specific energy in rock drilling. *Int. J. Rock. Mech. Min. Sci.* **2** (1), 57–73 (1965).
35. Zhang, Q. et al. Identification and optimization of energy consumption by shield tunnel machines using a combined mechanical and regression analysis. *Tunn. Undergr. Space Technol.* **28**, 350 (2012).
36. Wu, W. *Research on Stratum Identification Method Based on Shield Machine Excavation Parameters* (Shijiazhuang Tiedao University, 2023).
37. Zhan, R. et al. An improved equivalent heat capacity method to simulate and optimize latent thermal energy storage units. *Int. J. Heat Mass Trans.* **235**, 126135 (2024).

### Author contributions

HB. W. and GG. C.: formal and data analysis, methodology, project administration, validation, funding acquisition; Z. S. and L. Z.: investigation, data curation, writing—review & editing; CD. G. and ZW. D.: formal analysis, visualization, writing—original draft, writing—review & editing, funding acquisition.

### Declarations

### Competing interests

The authors declare no competing interests.

### Additional information

**Correspondence** and requests for materials should be addressed to C.G.

**Reprints and permissions information** is available at [www.nature.com/reprints](http://www.nature.com/reprints).

**Publisher's note** Springer Nature remains neutral with regard to jurisdictional claims in published maps and institutional affiliations.

**Open Access** This article is licensed under a Creative Commons Attribution-NonCommercial-NoDerivatives 4.0 International License, which permits any non-commercial use, sharing, distribution and reproduction in any medium or format, as long as you give appropriate credit to the original author(s) and the source, provide a link to the Creative Commons licence, and indicate if you modified the licensed material. You do not have permission under this licence to share adapted material derived from this article or parts of it. The images or other third party material in this article are included in the article's Creative Commons licence, unless indicated otherwise in a credit line to the material. If material is not included in the article's Creative Commons licence and your intended use is not permitted by statutory regulation or exceeds the permitted use, you will need to obtain permission directly from the copyright holder. To view a copy of this licence, visit <http://creativecommons.org/licenses/by-nc-nd/4.0/>.

© The Author(s) 2025